

AD-A097 708 MISSION RESEARCH CORP SANTA BARBARA CA F/G 18/3  
SUITABILITY OF ARES FOR SIMULATING TACTICAL BURST EMP ENVIRONME--ETC(U)  
APR 80 D W HOLST DNA001-80-C-0076  
UNCLASSIFIED MRC-R-565 DNA-5442T NL

F/G 18/3

APR 80 D W HOLST

DNA001-80-C-0076

NL

DNA-5442T

40 A  
097708

END  
DATE  
FILMED  
5-8  
DTIC

SECRET

12

DNA 5442T

AD A 097 708

# SUITABILITY OF ARES FOR SIMULATING TACTICAL BURST EMP ENVIRONMENTS

D. W. Holst  
Mission Research Corporation  
P.O. Drawer 719  
Santa Barbara, California 93101

1 April 1980

Topical Report for Period 15 January 1980—1 April 1980

CONTRACT No. DNA 001-80-C-0076

APPROVED FOR PUBLIC RELEASE;  
DISTRIBUTION UNLIMITED.

DTIC  
S  
APR 14 1981  
A

THIS WORK SPONSORED BY THE DEFENSE NUCLEAR AGENCY  
UNDER RDT&E RMSS CODE B323080464 X99QAXVC30102 H2590D.

DTIC FILE COPY

Prepared for  
Director  
DEFENSE NUCLEAR AGENCY  
Washington, D. C. 20305

81 4 14 008

Destroy this report when it is no longer  
needed. Do not return to sender.

PLEASE NOTIFY THE DEFENSE NUCLEAR AGENCY,  
ATTN: STTI, WASHINGTON, D.C. 20305, IF  
YOUR ADDRESS IS INCORRECT, IF YOU WISH TO  
BE DELETED FROM THE DISTRIBUTION LIST, OR  
IF THE ADDRESSEE IS NO LONGER EMPLOYED BY  
YOUR ORGANIZATION.



UNCLASSIFIED

SECURITY CLASSIFICATION OF THIS PAGE (When Data Entered)

REPORT DOCUMENTATION PAGE		READ INSTRUCTIONS BEFORE COMPLETING FORM
1. REPORT NUMBER DNA 5442T	2. GOVT ACCESSION NO. AD-AC47708	3. RECIPIENT'S CATALOG NUMBER
4. TITLE (and Subtitle) SUITABILITY OF ARES FOR SIMULATING TACTICAL BURST EMP ENVIRONMENTS.		5. TYPE OF REPORT & PERIOD COVERED Topical Report, <del>for</del> Period 15 Jan 80 - 1 Apr 80
7. AUTHOR D. W. Holst		6. PERFORMING ORG. REPORT NUMBER MRC-R-565
9. PERFORMING ORGANIZATION NAME AND ADDRESS Mission Research Corporation P.O. Drawer 719 Santa Barbara, California 93102		8. CONTRACT OR GRANT NUMBER(s) DNA 001-80-C-0076
11. CONTROLLING OFFICE NAME AND ADDRESS Director Defense Nuclear Agency Washington, D.C. 20305		10. PROGRAM ELEMENT, PROJECT, TASK AREA & WORK UNIT NUMBERS Subtask X99QAXVC301-02
14. MONITORING AGENCY NAME & ADDRESS (if different from Controlling Office)		12. REPORT DATE 1 Apr 1980
		13. NUMBER OF PAGES 72
		15. SECURITY CLASS. (of this report) UNCLASSIFIED
		15a. DECLASSIFICATION DOWNGRADING SCHEDULE
16. DISTRIBUTION STATEMENT (of this Report)  Approved for public release; distribution unlimited.		
17. DISTRIBUTION STATEMENT (of the abstract entered in Block 20, if different from Report)		
18. SUPPLEMENTARY NOTES  This work sponsored by the Defense Nuclear Agency under RDT&E RMSS Code B323080464 X99QAXVC30102 H2590D.		
19. KEY WORDS (Continue on reverse side if necessary and identify by block number)  <div style="display: flex; justify-content: space-between;"> <div> ARES Source Region Coupling </div> <div> Simulation Tactical System EMP </div> </div>		
20. ABSTRACT (Continue on reverse side if necessary and identify by block number) The possibility of using the ARES to evaluate source region coupling in tactical systems is discussed. A "tactical" source region is defined and the environment at the inner edge of this source region is determined for a 50 kt burst at a range of 1.2 km. The time and amplitude characteristics of the ARES pulse are compared with those from the selected environment. Coupling of the ARES and the source region fields into a short monopole antenna and small loop are compared. These objects are representative of those found.		

DD FORM 1473

1 JAN 73

EDITION OF 1 NOV 65 IS OBSOLETE

UNCLASSIFIED

SECURITY CLASSIFICATION OF THIS PAGE (When Data Entered)

UNCLASSIFIED

SECURITY CLASSIFICATION OF THIS PAGE(When Data Entered)

20. ABSTRACT (Continued)

in tactical systems. Based upon these results suggestions are made for augmenting and supplementing testing in the ARES to obtain responses representative of the source region.

UNCLASSIFIED

SECURITY CLASSIFICATION OF THIS PAGE(When Data Entered)

## PREFACE

The author wishes to express thanks to Dr. William Crevier for providing much of the source region data and for many helpful discussions throughout the course of this work. Mr. Robert Hamilton provided the Fourier transforms and time derivatives for the source region and ARES data.

Approved For	
SECRET	X
Classification	
Declassify on	
A	

## TABLE OF CONTENTS

<u>SECTION</u>	<u>PAGE</u>
PREFACE	1
LIST OF ILLUSTRATIONS	3
1 INTRODUCTION	5
2 THE SOURCE REGION ENVIRONMENT	10
2.1 TYPICAL ENVIRONMENT	11
2.2 ARES EMP ENVIRONMENT	21
3 SOURCE REGION COUPLING	34
3.1 COUPLING MODIFICATION IN THE SOURCE REGION ENVIRONMENT	36
3.2 COUPLING TO CANONICAL OBJECTS	39
3.2.1 Short Monopole Antenna	39
3.2.2 Small Loop Antenna	45
4 ARES MODIFICATIONS FOR SOURCE REGION TESTS	52
5 SUMMARY AND CONCLUSIONS	57
REFERENCES	62

## LIST OF ILLUSTRATIONS

<u>FIGURE</u>		<u>PAGE</u>
1-1	ARES facility description.	7
1-2	Coordinate system for ARES.	8
2-1	Variation of the peak Compton current $J_r$ with range for a 50 kt surface burst.	12
2-2	Variation of the peak electric and magnetic fields with range for a 50 kt surface burst.	13
2-3	Variation of the peak air conductivity $\sigma$ with range for a 50 kt surface burst.	14
2-4	Radial Compton current vs time at 1.2 km from a 50 kt surface burst.	16
2-5	Electric and magnetic fields vs time at 1.2 km from a 50 kt surface burst.	18
2-6	Air conductivity vs time at 1.2 km from a 50 kt surface burst.	19
2-7	Source region displacement current and conduction current densities at 1.2 km from a 50 kt surface burst.	20
2-8	Comparison of horizontal magnetic fields for the ARES and source region.	23
2-9	Comparison of vertical electric fields for the ARES and source region.	24
2-10	Comparison of longitudinal electric fields for the ARES and source region.	25
2-11	Time derivative of the vertical electric field for the ARES and source region showing relative magnitudes.	27
2-12	Time derivative of the horizontal magnetic field for the ARES and source region showing relative magnitudes.	28



## LIST OF ILLUSTRATIONS (continued)

<u>FIGURE</u>	<u>PAGE</u>
2-13 Fourier transform of magnetic field for ARES and for source region.	29
2-14 Fourier transform of vertical electric field for ARES and for source region.	30
2-15 Fourier transform of longitudinal electric field for ARES and for source region.	31
2-16 Conduction current and displacement current densities showing relative magnitudes.	33
3-1 Typical coupling elements for deployed tactical systems.	35
3-2 Equivalent circuit for short monopole in the source region.	41
3-3 Response of a short antenna 1.2 km from a 50 kt surface burst.	44
3-4 Response of a short antenna 2.0 km from a 50 kt surface burst.	46
3-5 Comparison of short antenna response in ARES and source region environments.	47
3-6 Equivalent circuit for small loop in the source region.	49
3-7 Comparison of small loop response in ARES and source region environments.	50

## SECTION 1

### INTRODUCTION

The ARES (Advanced Research Electromagnetic Simulator) is a parallel-plate transmission line simulator which provides a working volume 33 meters long by 40 meters wide by 40 meters high. It was originally designed and constructed to provide a free space (plane wave) EMP environment for the testing of full scale missiles in simulated flight.

This report considers application of the ARES to source region testing near the air-ground interface. Since the ARES was designed with a very different problem in mind, it is reasonable to anticipate that this new application will require some modification of the facility. Before the nature of these changes, if any, can be defined we must first determine to what extent the present ARES configuration compares with a typical source region environment. Some elements of the source region environment, such as air conductivity, will be missing entirely. Other parameters may be present but of incorrect sense or amplitude. The impact of the missing or modified parameters must be assessed. For the purposes of this report it was deemed best to choose a "typical" source region environment. This approach allows specific comparisons to be made, and can result in specific recommendations for modifications.

A major attribute of the ARES is its large physical size, allowing for the possibility of testing large tactical systems or components - vans, vehicles, towers, with their numerous cable interconnections.

Figure 1-1 provides a schematic representation of the ARES facility. All dimensions are in meters. The working volume is accessible via a surface road so that large vehicles and system components have direct access to the working floor space. Figure 1-2 shows the coordinate system employed for past field maps of the ARES working volume. The same coordinate system will be employed in this report to facilitate comparisons with previous work.

While a fully deployed tactical system covers considerably more territory than available in the ARES, major elements of a system could conceivably be tested under deployed conditions. For example, a communications and control van, a missile launcher, and their associated cabling and/or antennas might be arranged in the available ARES floor space to simulate a realistic deployment. Due to this unique capability the balance of this report will place emphasis on large tactical systems in the source region environment. Smaller systems or components can be tested in other simulators, such as AURORA, which are already operated as source region simulators but lack the large volume capability.

A previous study of the ARES as a source region simulator has been conducted by HDL<sup>1</sup>. In that study, the ARES is accepted for what it is, a plane wave simulator, and the comparison of the ARES and the source region environments is conducted at a range sufficiently far from the burst point that  $E_\theta$  and  $B_\phi$  have their free field ratio of the speed of light, or equivalently, that the air conductivity is small ( $\sigma < 10^{-6}$  mho/m).

It is felt that the above approach may be overly-restrictive and in this report we adopt a different viewpoint. Rather than concentrating on the outer edge of the source region, we will concentrate on the inner

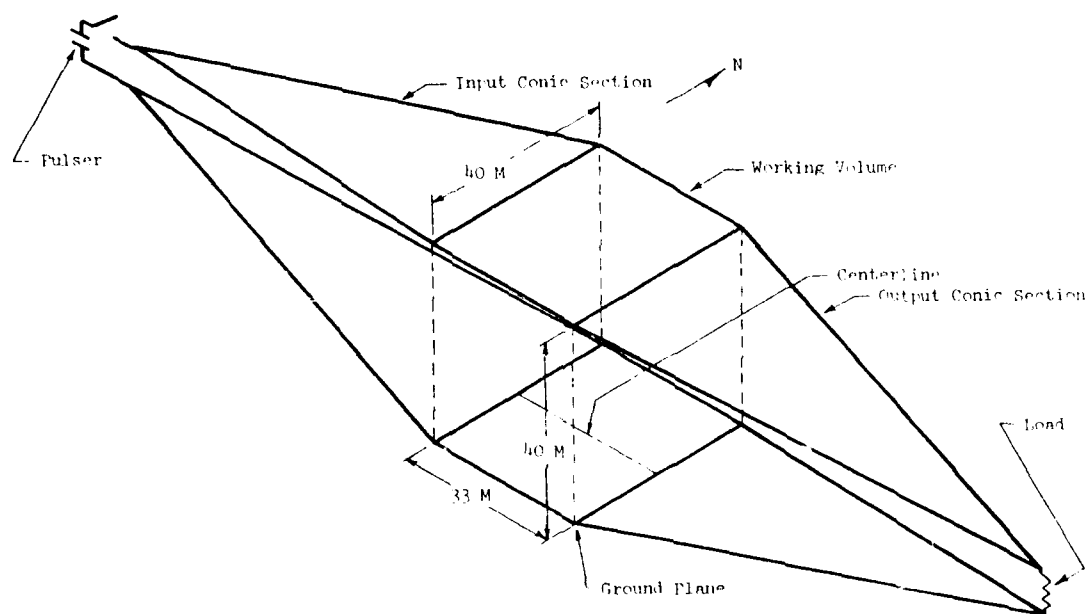


Figure 1-1. ARES facility description.

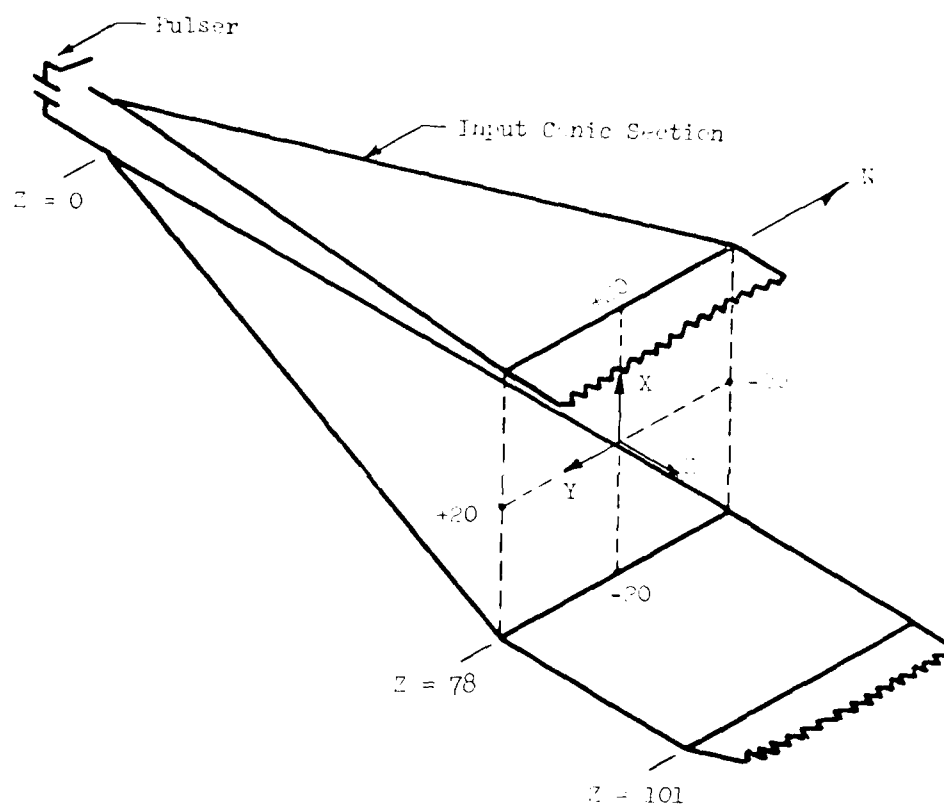


Figure 1-2. Coordinate system for ARES.

edge of the tactical source region - the minimum range at which crew survival is insured. Then equipment survival is also necessary for mission completion. This is the range for which our environment comparisons and coupling calculations were conducted. The EMP fields at this range are not plane wave, nor are the air conductivity and Compton currents insignificant. However, a plane wave simulator may still provide useful test results and this possibility should be examined in greater detail.

The comparisons described in later sections were conducted for a device with a 50 kT yield, with 3 percent of the yield in immediate neutron and gamma radiation. This is felt to be a reasonable upper limit for tactical nuclear weapons. The immediate dose from this device determines the crew survival range.

## SECTION 2

### THE SOURCE REGION ENVIRONMENT

Before proceeding with the technical discussion, we need to define what constitutes the "source region of interest". This is partly a philosophical and partly a physical definition since it must be guided by the prevailing battlefield philosophy as well as by the laws of physics.

The basic Army philosophy regarding nuclear survivability is that the particular item of equipment or system should survive if a sufficient percentage of its crew survives long enough to complete the mission<sup>2</sup>. Equipment failures can be generated by several nuclear weapon effects such as air blasts, thermal radiation, and EMP. In this report we will be concerned with how one verifies experimentally that an Army tactical system is hard to source region EMP. The air blast and thermal radiation, as well as total radiation dose, serve to define an inner radius to the source region since they would disable any crew located nearer the burst point.

The definition of the inner edge of the source region is somewhat arbitrary. It depends upon the type of protection a system provides the crew from nuclear weapon effects. The Army specifically considers: exposed personnel, personnel in foxholes, personnel in armored vehicles, and personnel in wheeled vehicles. It also depends upon the weapon output to which one expects to be exposed. The relative magnitudes of the various disabling mechanisms can vary greatly with weapon design.

In addition the EMP is sensitive to such parameters as the water content of the air, soil conductivity, and terrain features such as hills and valleys. It can also be modified by previous nuclear explosions.

## 2.1 TYPICAL ENVIRONMENT

In spite of the variability in the source region EMP it is useful to define a specific environment to which one may refer. Therefore, let us consider 50 kT yield as an upper limit for weapons of tactical interest. Assume that 3 percent of the yield is in initial neutron and  $\gamma$ -radiation.<sup>3</sup> A typical mean free path ( $\lambda$ ) at sea level for such radiation is  $3 \times 10^4$  cm. Using the fact that 1 kT equals  $4.18 \times 10^{19}$  ergs, 1 rad = 100 ergs/gm, and the density of air is  $\rho = 1.23 \times 10^{-3}$  gm/cm<sup>3</sup>, we find that the immediate dose at a radius  $r$  is

$$D = \frac{Y \times 0.03 \times 4.18 \times 10^{19} e^{-r/\lambda}}{100 \times 4\pi r^2 \times \rho \lambda}$$

$$D = 1.35 \times 10^{15} e^{-r/\lambda} / r^2 \text{ rads}$$

At  $r = 10^5$  cm,  $D = 4800$  rads, while at  $r = 1.5 \times 10^5$ ,  $D = 405$  rads. Doses in the 1000 to 5000 rad range produce almost immediate incapacitation<sup>3</sup> so we may define the inner radius of the source region to be somewhere in the 1 to 1.5 km range.

Figures 2-1 through 2-3 display the variation in the peak values of the radial Compton current,  $J_r$ , the radial electric field,  $E_r$ , the azimuthal magnetic field,  $B_\phi$ , the vertical electric field,  $E_\theta$ , and the air conductivity,  $\sigma$ , with range for a 50 kT surface burst. All values are



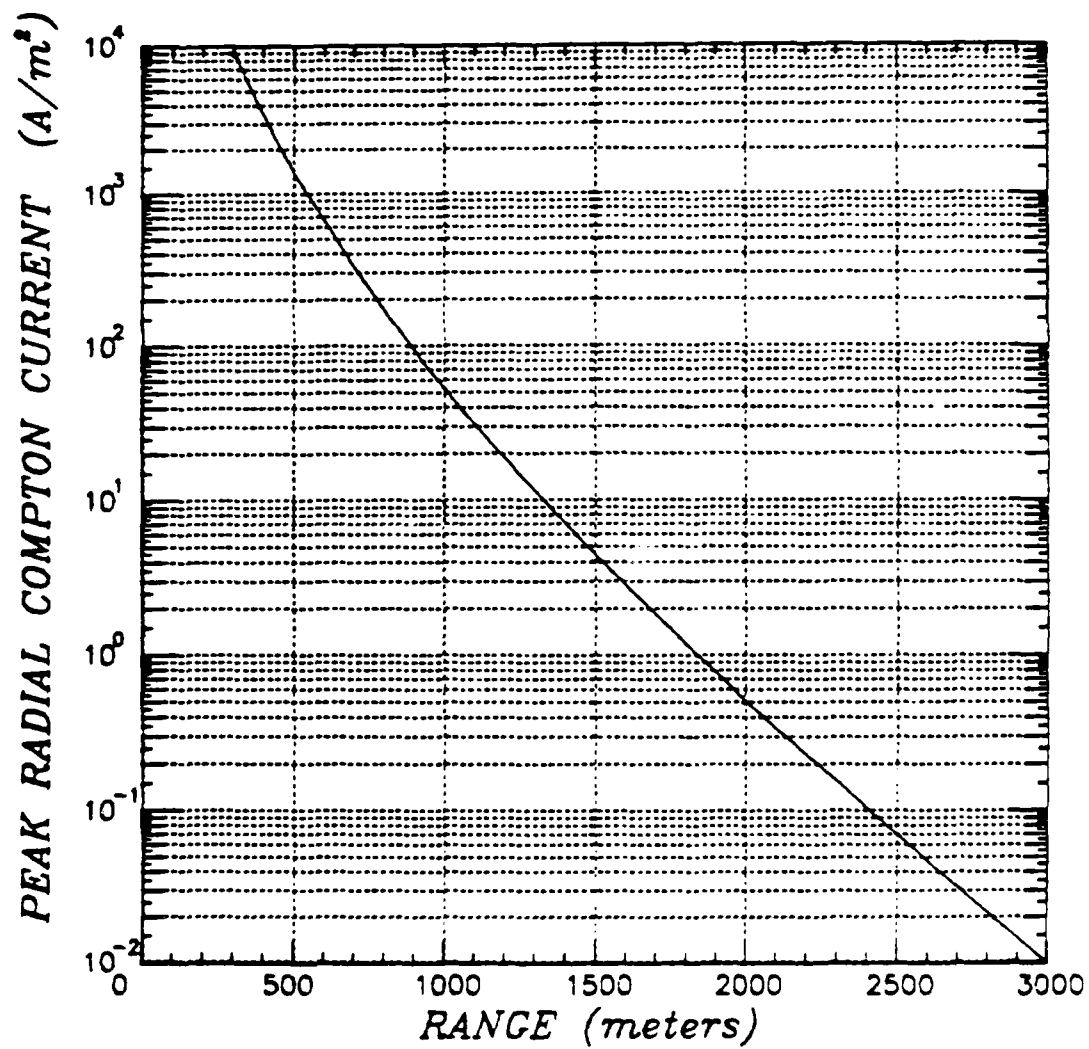


Figure 2-1. Variation of the peak Compton current  $J_r$  with range for a 50 kt surface burst. The Compton current is in the negative r-direction.

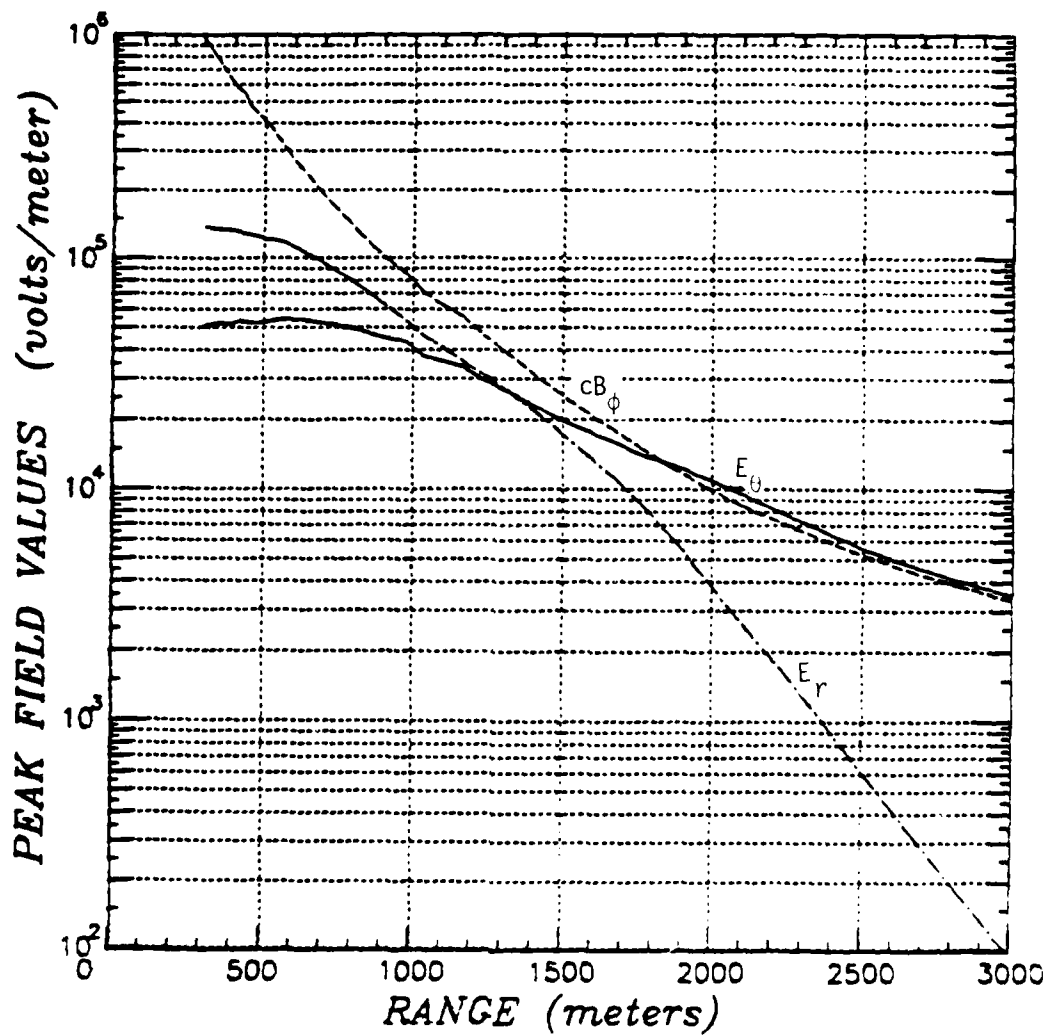


Figure 2-2. Variation of the peak electric ( $E_r, -E_\theta$ ) and magnetic ( $-cB_\phi$ ) fields with range for a 50 kt surface burst.

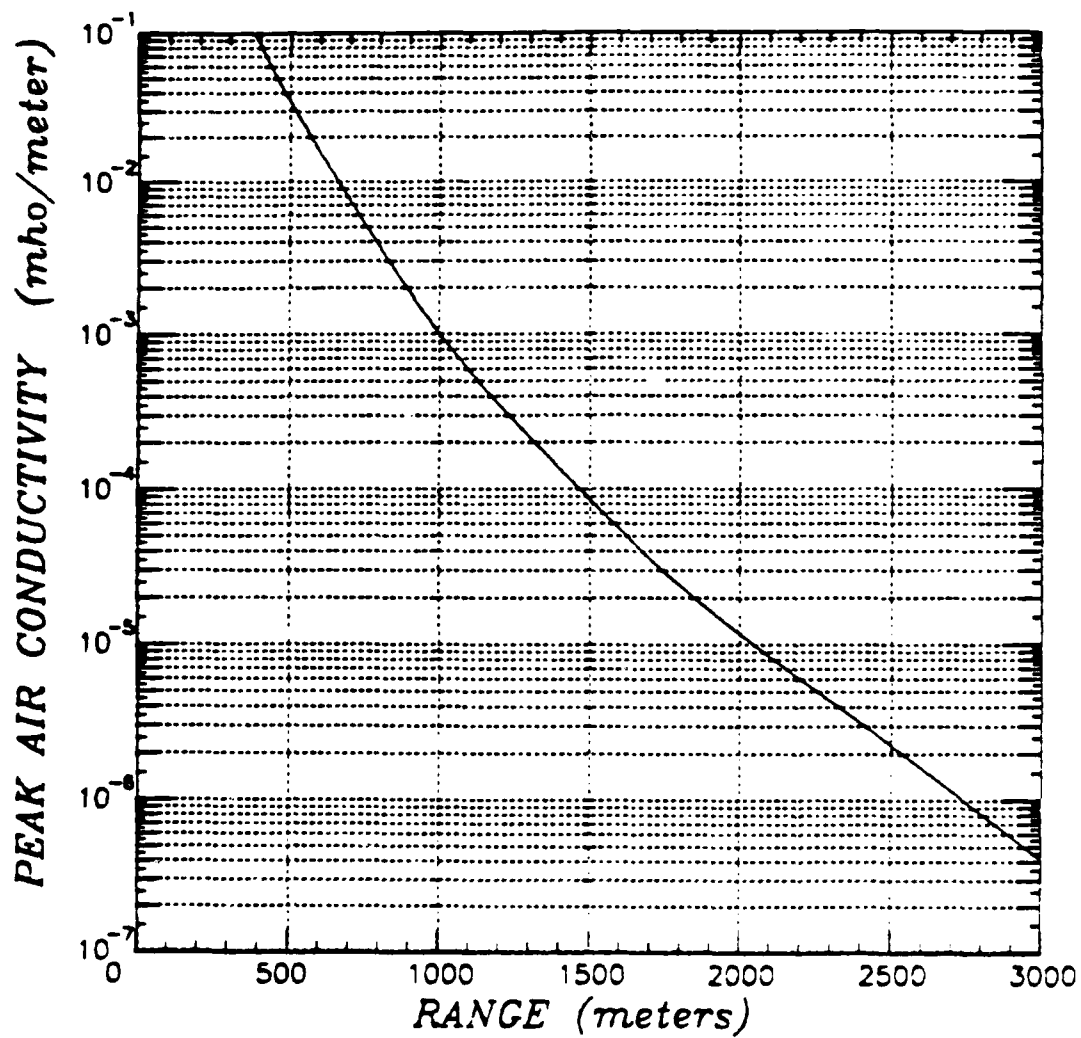


Figure 2-3. Variation of the peak air conductivity with range for a 50 kt surface burst.

near the ground-air interface. Results are from the new MRC/HDL code MODEL C which assumes a perfectly conducting ground. A one percent air moisture content was assumed.

Figure 2-1 shows that in the 1 to 1.5 km range of interest the radial current decreases from 55 to 4.5 amps/m<sup>2</sup>. The resulting radial electric field  $E_r$  varies from 50 to 18 kV/meter. The vertical gradient in the radial electric field at the ground results in the generation of  $B_\phi$  and  $E_\theta$  field components. It is seen that  $B_\phi$  varies from about  $2.8 \times 10^{-4}$  to about  $10^{-4}$  Tesla over the ranges of interest. The magnetic field is plotted as  $cB_\phi$  (in kV/m) in Figure 2-2 to emphasize the distinction between the source region and plane wave propagation. The fields become essentially plane wave when  $E_\theta = cB_\phi$  at about 1.8 km. The vertical electric field shows less variation ranging from about 40 to 20 kV/meter. The air conductivity changes from  $10^{-3}$  to  $10^{-4}$  mho/meter over the 1.0 to 1.5 km range.

For the following discussion we select a range of 1.2 km from the burst point. The immediate dose at this range is estimated to be 1720 rads. We therefore proceed to define a specific environment under the following assumptions:

- (a) Surface burst
- (b) 50 kT yield
- (c) Range from burst = 1.2 km
- (d) Perfectly conducting ground
- (e) Air moisture content = 1 percent
- (f) Air density =  $1.23 \times 10^{-3}$  gm/cm<sup>3</sup>

The EMP environment parameters at our designated range are defined by Figures 2-4 through 2-6 which present computed time histories. The Compton current, shown in Figure 2-4, has an initial e-folding time of  $10^{-8}$  sec.

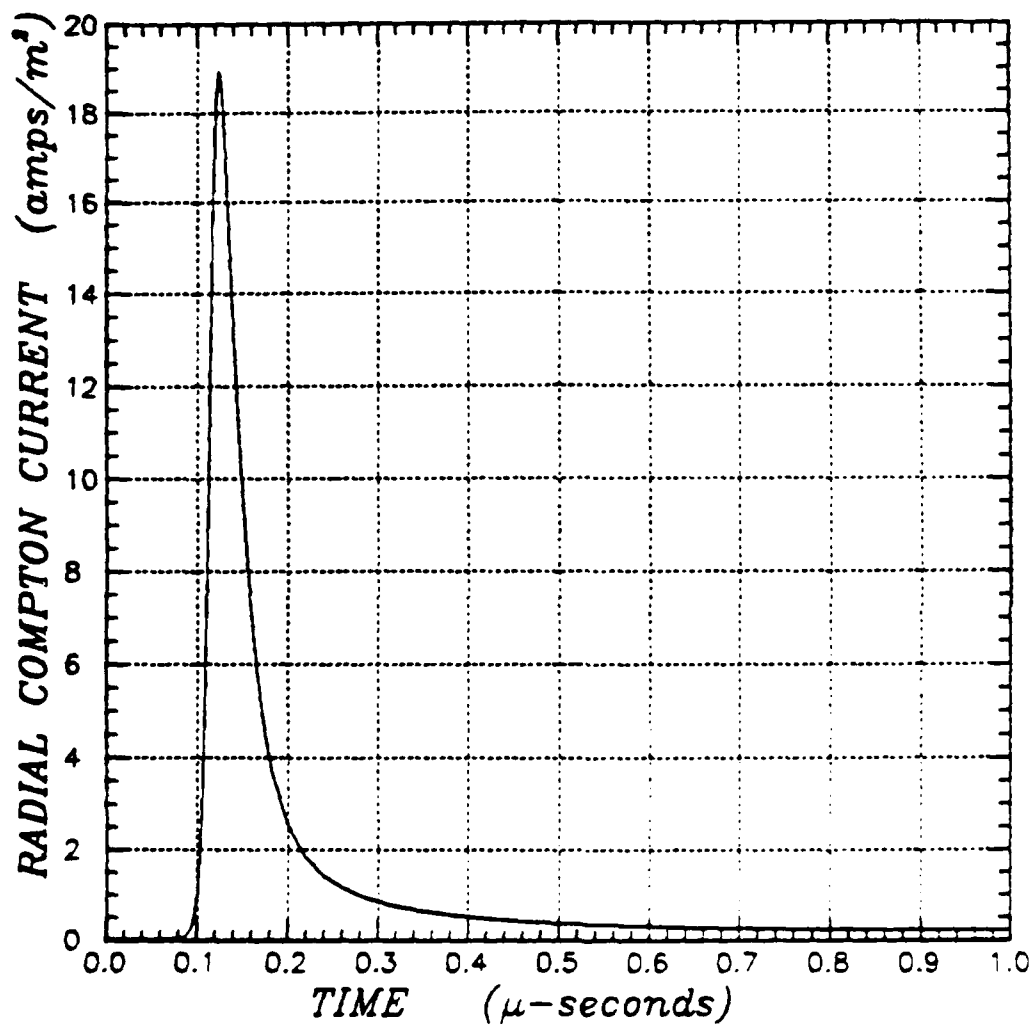


Figure 2-4. Radial Compton current versus time at 1.2 km from a 50 kt surface burst. The radial component of the Compton current is negative.

At  $4 \times 10^{-8}$  sec it decreases to  $5 \times 10^{-9}$  seconds. The peak current is about 19 A/m which occurs at  $1.2 \times 10^{-7}$  seconds.

The assumption of a perfectly conducting ground causes the radial electric field to be shorted out so that  $E_r = 0$  there. However, at relatively short distances above the ground ( $\approx 3$  meters)  $E_r$  is not zero but is given in Figure 2-5. The peak value is about 34 kV/meter, dropping to a relatively constant value of 15 kV/meter for later times.

Figure 2-5 shows that the surface magnetic field continues to rise beyond the peak in the Compton current. It eventually reaches a maximum value of about  $1.8 \times 10^{-4}$  Tesla which corresponds to an H of 143 A/m. It should be noted that  $B_\phi$  is negative. This corresponds to a positive surface current that is flowing radially outward or an electron flow back towards the burst point.

The vertical electric field in Figure 2-5 points upward at the surface which corresponds to a negative  $E_\theta$ . At the peak of the Compton current  $E_\theta$  also peaks. It continues decreasing until  $4 \times 10^{-7}$  seconds when it begins increasing again. By 10  $\mu$ seconds it has increased to nearly the value it had at the peak of the prompt  $\gamma$ -pulse.

Air conductivity versus time is shown in Figure 2-6. The air conductivity peaks at about  $3.5 \times 10^{-4}$  mho/m, just after the peak in the Compton current. By 10  $\mu$ seconds it has fallen to about  $10^{-5}$  mho/m. Because of the air conductivity both conduction ( $\sigma E$ ) and displacement ( $\epsilon_0 \dot{E}$ ) current densities are present in the source region. These two currents are presented in Figure 2-7 with the displacement current labeled D (solid curve) and the conduction current labeled C (dashed curve). They are seen to dominate at different times, reaching comparable peak magnitudes.

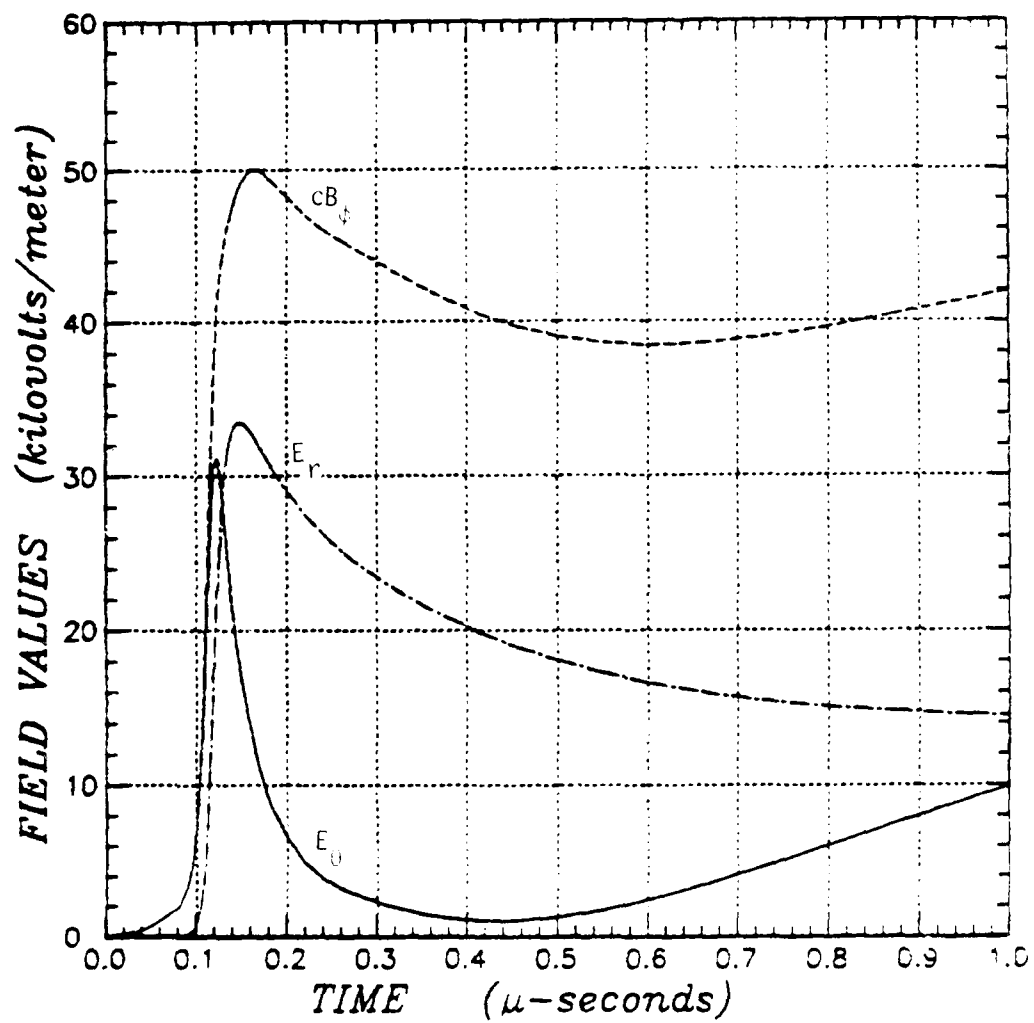


Figure 2-5. Electric ( $E_r$ ,  $E_\theta$ ) and magnetic ( $-cB_z$ ) fields versus time at 1.2 km from a 50 kt surface burst. Note that the scale is in kilovolts/meter.

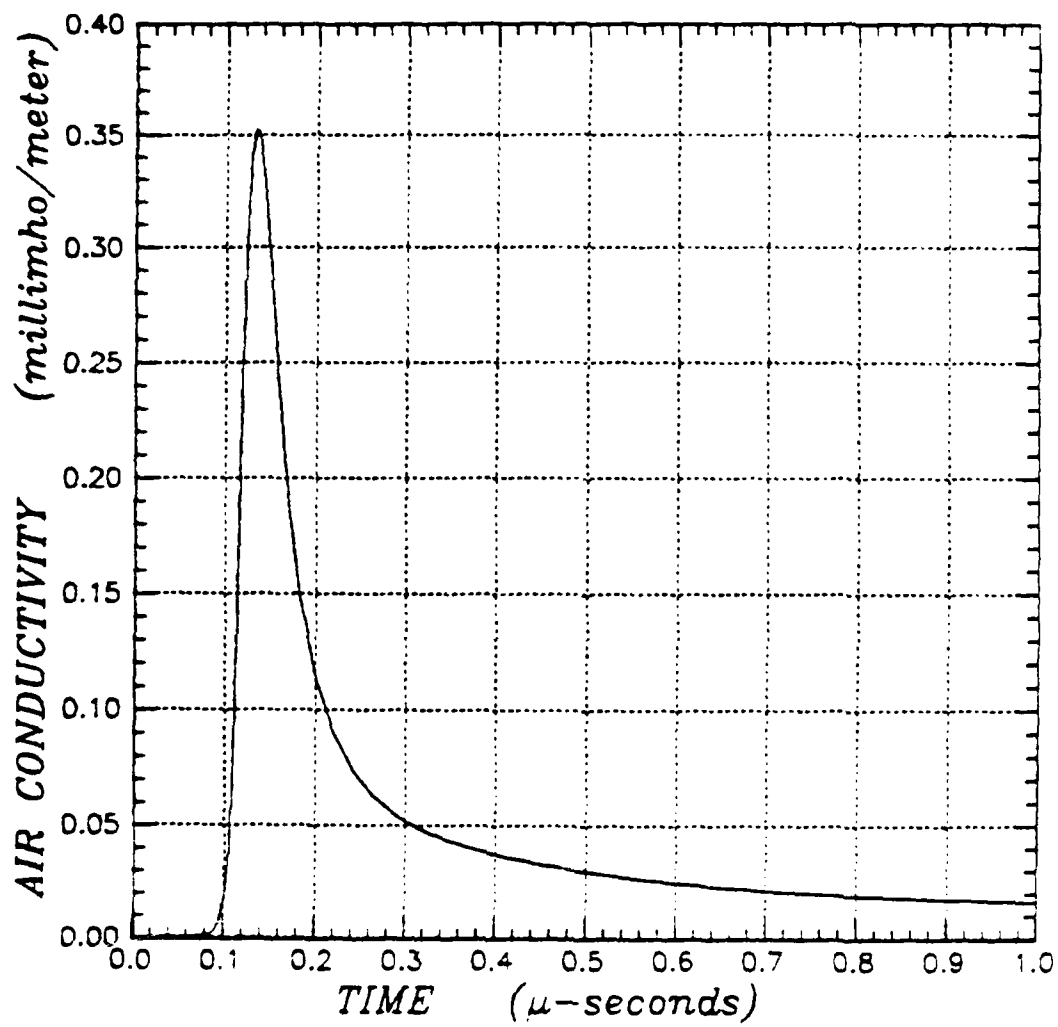


Figure 2-6. Air conductivity versus time at 1.2 km from a 50 kt surface burst. Note that the scale is in millimho/meter.



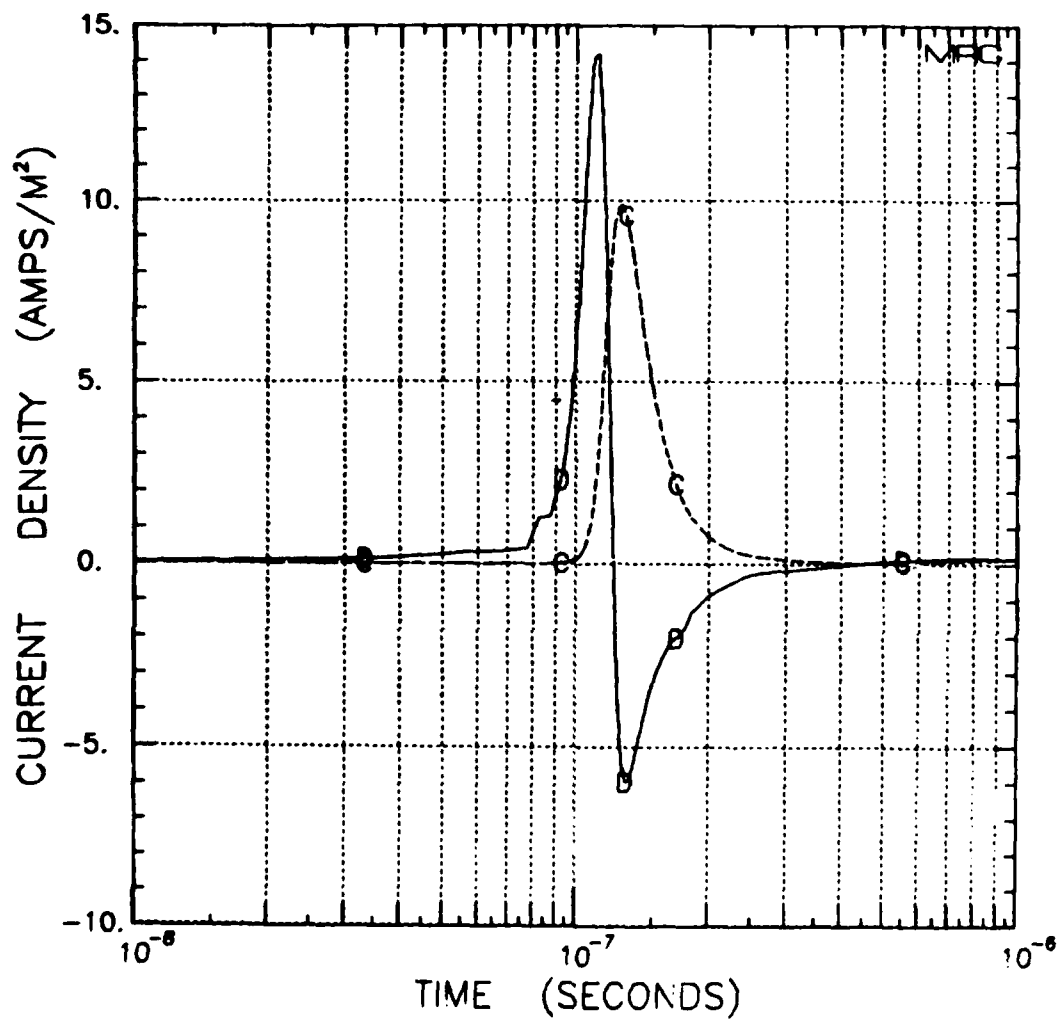


Figure 2-7. Source region displacement current ( $-\epsilon_0 \dot{E}_\theta$ ) and conduction current ( $-\sigma E_\theta$ ) densities at 1.2 km from a 50 kt surface burst.

It should be noted that the ARES provides the correct fields in terms of components present and sense, though amplitudes differ. For example, the ARES  $E_x$  corresponds to the source region  $-E_\theta$  since the source region vertical electric field is negative in the spherical coordinate system (points upward). Similarly, we have  $E_z = -E_R$  and  $B_y = -B_\phi$ . Because of this one-for-one correspondence, the ARES field designations  $E_x$ ,  $B_y$ ,  $E_z$  (see Figure 1-2) will be adopted throughout the remainder of this report.

Adaptation of the ARES as a source region simulator must be examined in terms of the source region environment generated by a nuclear surface burst. Physical descriptions of the source region, which elaborate upon the characteristics described above, may be found in References 4 and 5.

## 2.2 ARES EMP ENVIRONMENT

In the previous section the source region environment 1.2 km from a 50 kt burst has been defined in terms of the time histories of several source and field parameters. Comparisons between the ARES and the source region defined above have been conducted for several environment parameters with the results summarized in Figures 2-8 to 2-16.

ARES data were obtained from References 6 through 9. Basically, the ARES is a parallel plate transmission line simulator with conical input and output sections. It operates in the TEM mode, with  $E_x$  and  $B_y$  the principal electric and magnetic field components respectively. Due to spherical wave, diffraction and reflection effects a longitudinal ( $E_z$ ) electric field component is present and the propagation velocity is about 8 percent below the velocity of light (the wave impedance is not quite plane wave). The ARES coordinate system is shown in Figure 1-2.

For the parameter comparisons presented below the time plot for the measured ARES magnetic field,  $B_y$ , was employed.<sup>9</sup> The  $E_x$  and  $E_z$  electric field time variations were assumed to be the same with amplitude adjustments to fit measured peak values.<sup>7</sup>

Comparisons of the pulse time histories for the ARES and the source region are presented in Figures 2-8 to 2-10. The ARES is shown as the solid line with a dashed line for the source region. The magnitude of  $E_x$  in the ARES exceeds the source region amplitude by about 70 percent. The peak magnitude of  $E_z$  in the ARES is only about 30 percent of the source region value but the peak amplitudes of the  $B_y$ 's are nearly identical.

The ARES pulser is capable of providing a very fast rise time with typical values between 5 and 10 ns. The source region pulse shows an e-folding with  $\alpha \approx 2 \times 10^8/\text{sec}$ . This parameter depends upon the device, burst altitude and ground conductivity but the value shown here is not untypical. With a 10-90 percent rise time of 10 ns the ARES provides a very good simulation of the leading edge of the source region pulse.

For late times the source region fields maintain high amplitudes, except for  $E_x$  which first shows a rapid drop after the peak before again climbing to its peak value. By  $10^{-3}$  seconds all field components have decreased to small values. The ARES fields drop rapidly after the peak, providing a reasonably good simulation of the early time vertical electric field but showing no correspondence to the field components for late times. It will be seen in the next section, however, that the coupling response is often more sensitive to  $\dot{E}$  and  $\dot{B}$ , the time derivatives of the electric and magnetic fields, than to the field components proper. We should therefore examine the time derivatives to evaluate their impact on the source region simulation.

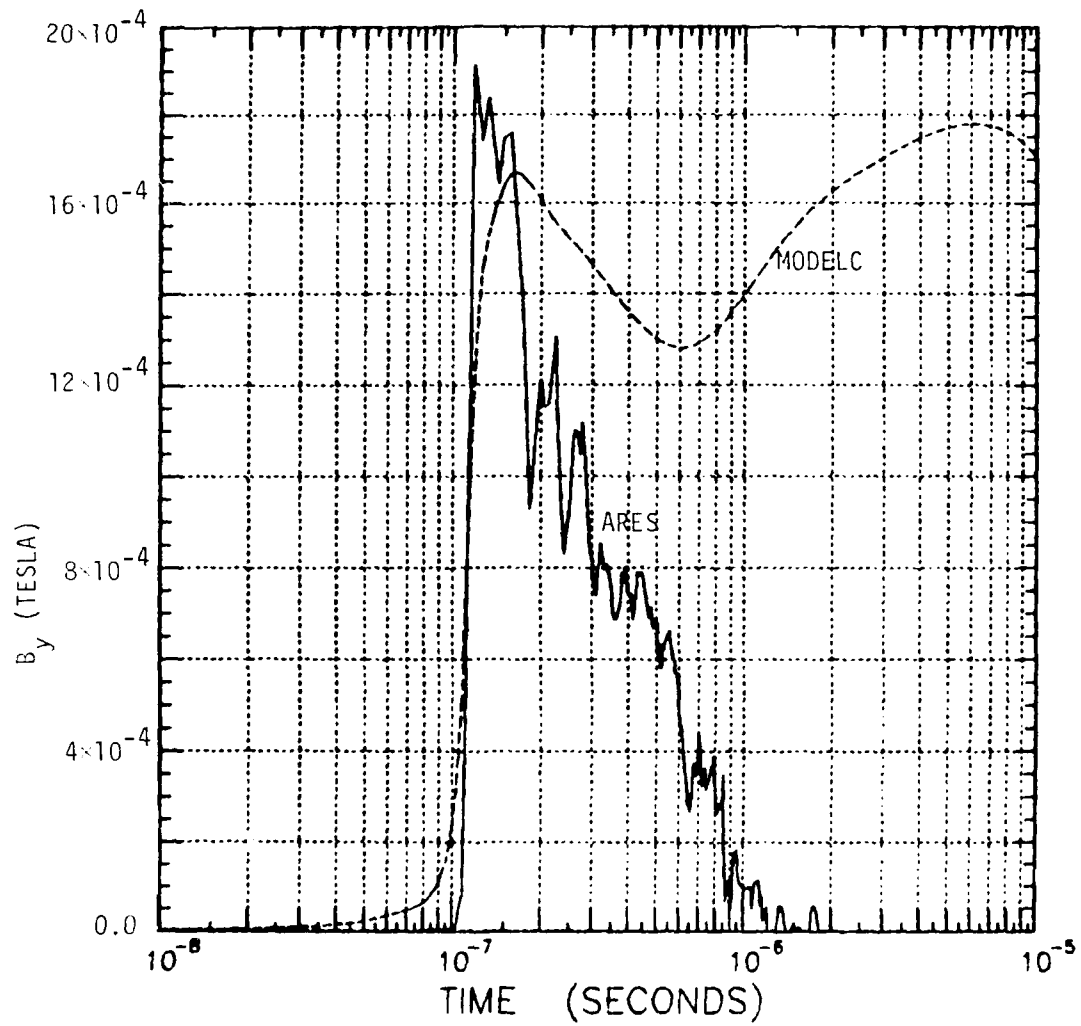


Figure 2-8. Comparison of horizontal magnetic fields for the ARES and source region.

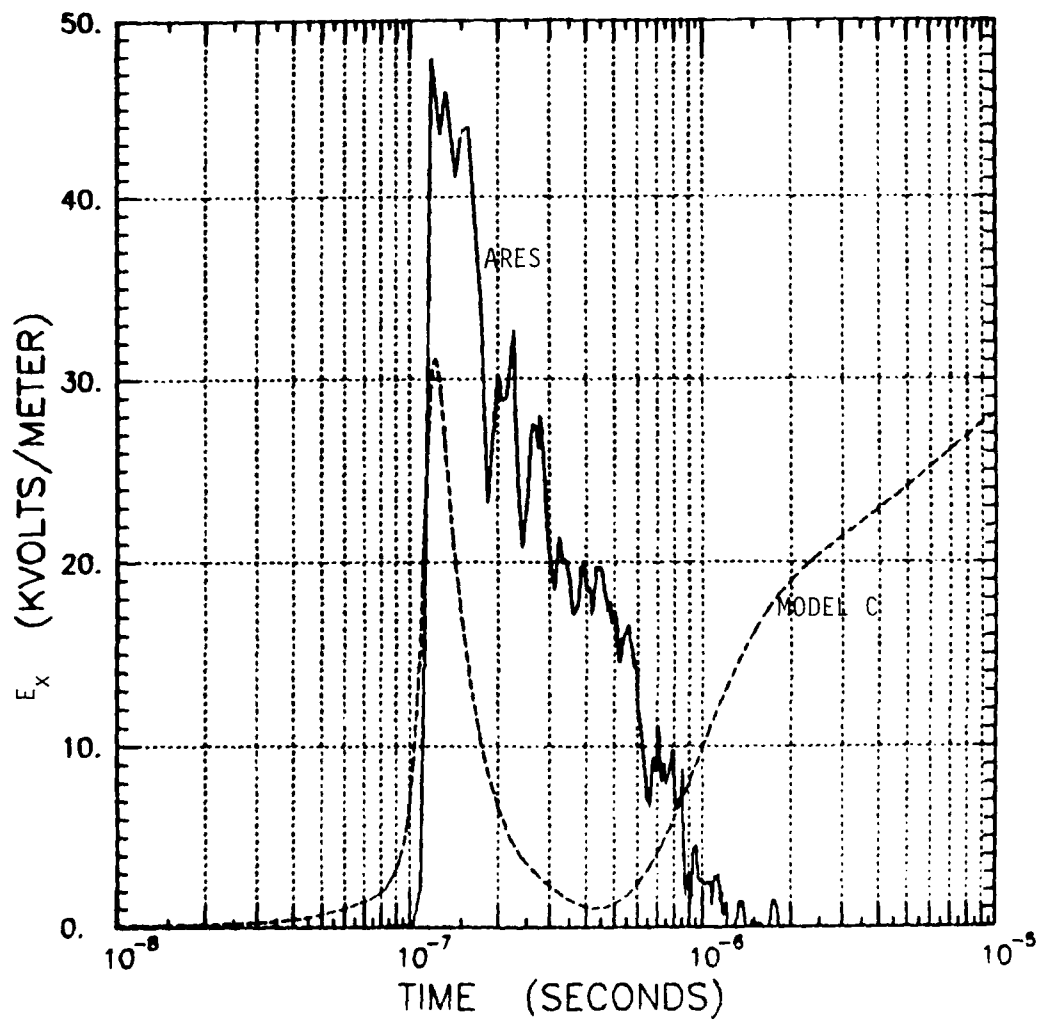


Figure 2-9. Comparison of vertical electric fields for the ARES and source region. Note that the scale is kilovolts/meter.

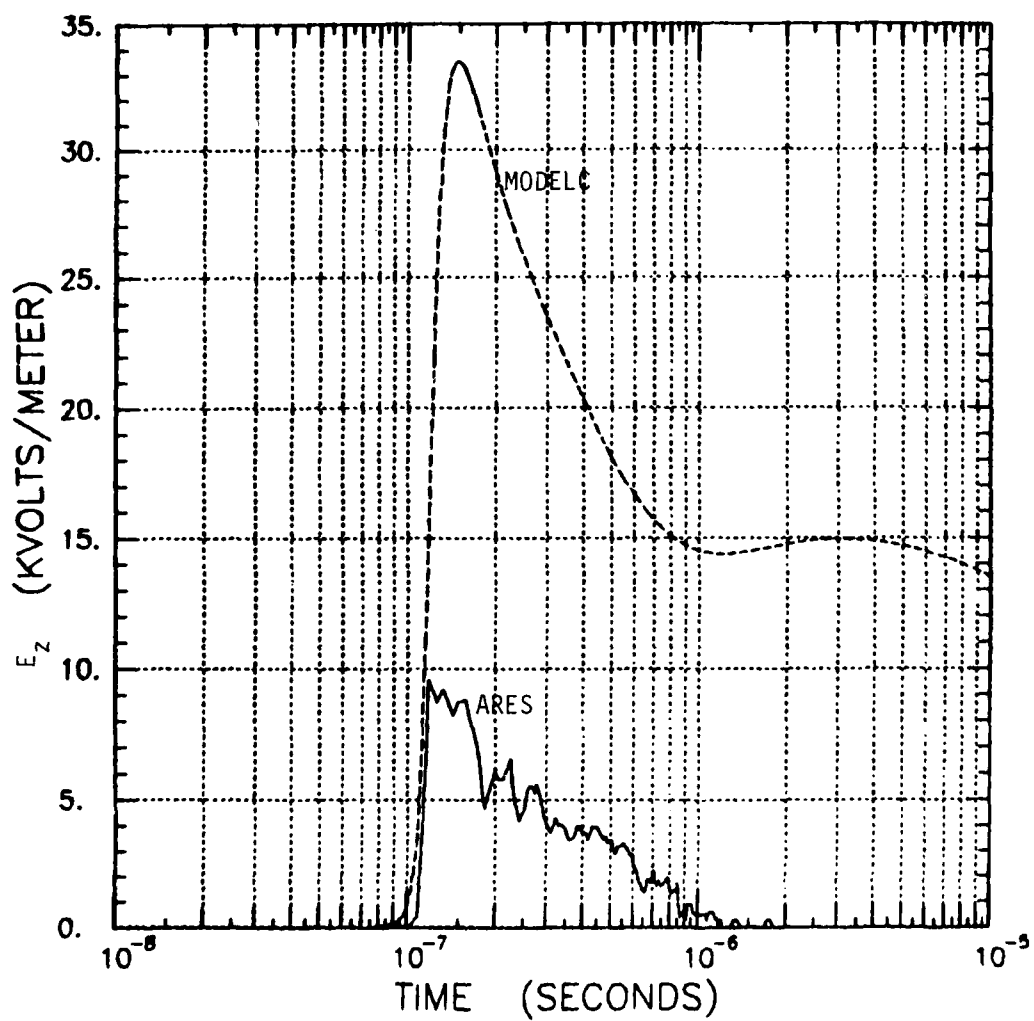


Figure 2-10. Comparison of longitudinal electric fields for the ARES and source region. Note that the scale is kilovolts/meter.

Time derivatives of  $E_x$  and  $B_y$  are presented in Figures 2-11 and 2-12, shown by a dashed line. They were computed using the source region results from the MODEL C code. The ARES results are presented on each plot as a solid line. It is seen that the magnitudes for the ARES exceed the source region values by a factor of six for both  $\dot{E}_x$  and  $\dot{B}_y$  providing a significant margin of overtest capability. Since dipoles and loops respond primarily to  $\dot{E}_x$  and  $\dot{B}_y$  respectively, the figures show the relative amplitudes of drives for these elements in the ARES and source region. For the  $\dot{E}_x$  negative overshoot, the ARES exceeds the MODEL C value by nearly a factor of 2.

Fourier transforms of all field components are presented in Figures 2-13 to 2-15. In each figure the ARES is represented by a solid line and the source region by a dashed line. The ARES transforms were obtained from the time histories shown in Figures 2-8 to 2-10. They show the characteristic notches at 17 and 34 MHz and in general are the same as transforms shown in the references.<sup>7,9</sup> For all field components the ARES shows higher amplitudes at high frequencies and lower amplitudes at low frequencies. It will therefore provide an overtest capability at high frequencies where many system components show the greatest coupling response.

Since the source region field amplitudes generally remain high to late times the transforms show higher amplitudes at low frequencies. This is particularly true for the radial electric field  $E_z$  which has a large amplitude in the source region (see Figure 2-10). The net result is that the ARES provides an overtest at high frequencies and an undertest at low frequencies. The crossover frequency between undertest and overtest is different for each field component, being 2 MHz for the horizontal magnetic field, 180 KHz for the vertical electric field, and 50 MHz for

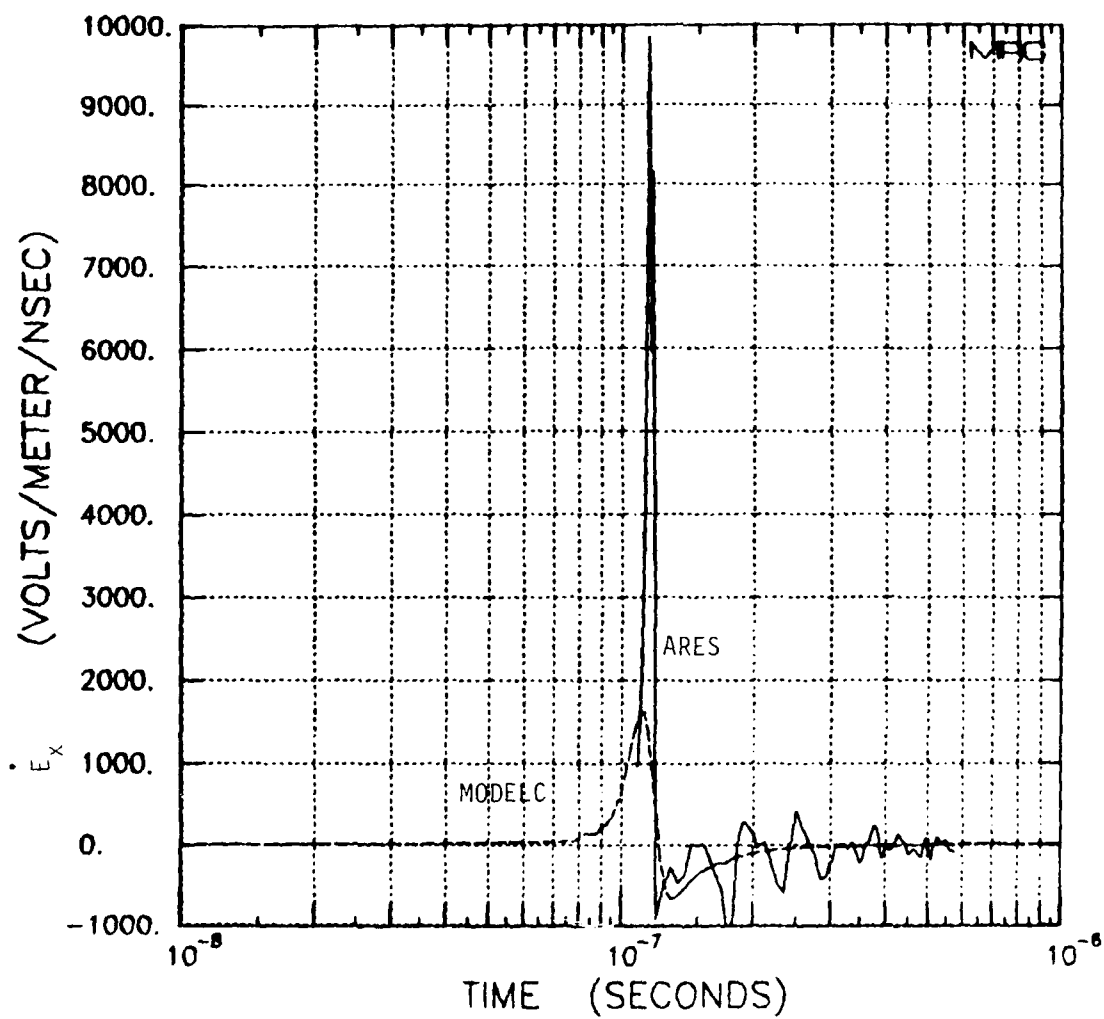


Figure 2-11. Time derivative of the vertical electric field ( $\dot{E}_x$ ) for the ARES and source region showing relative magnitudes. Note that the vertical scale is volts/meter/nanosecond.



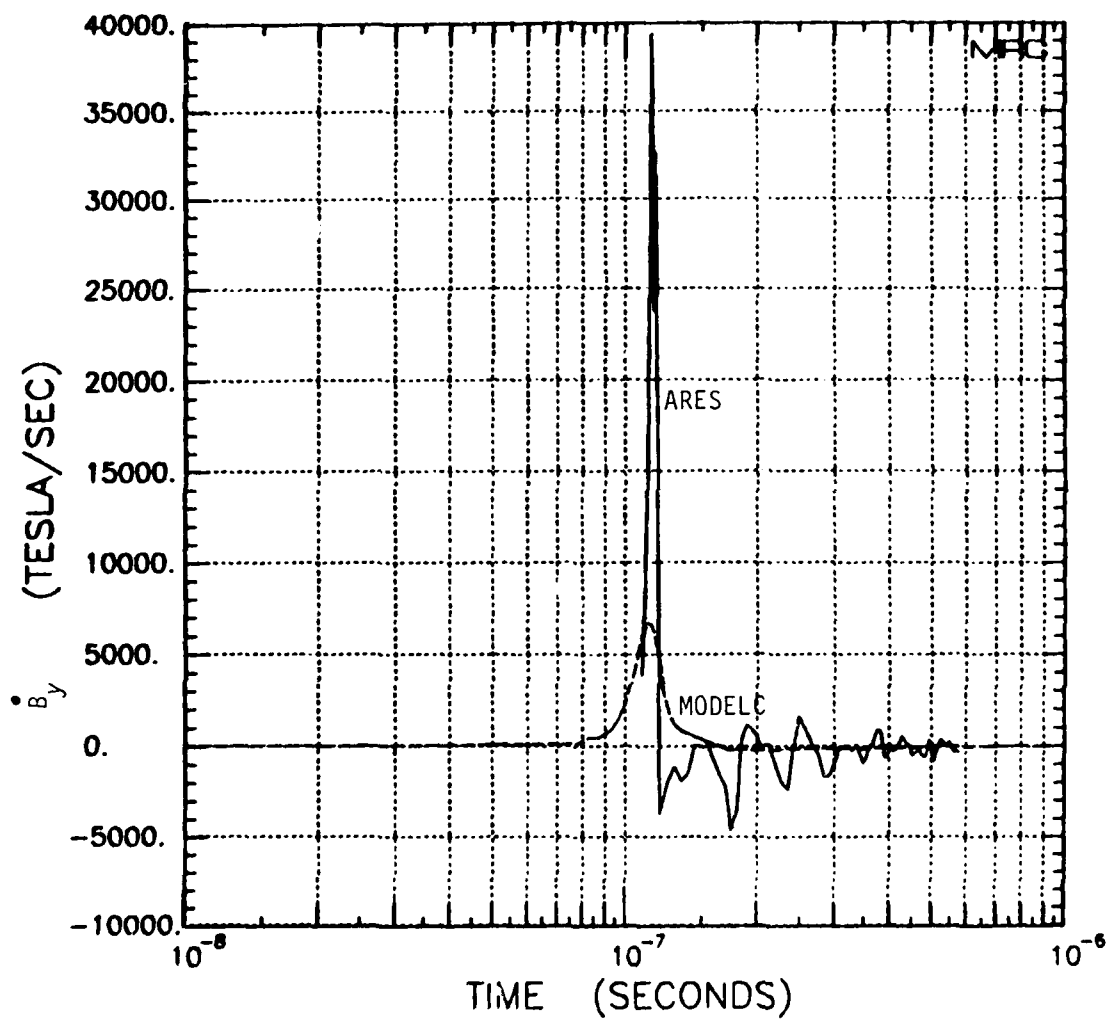


Figure 2-12. Time derivative of the horizontal magnetic field ( $\dot{B}_y$ ) for the ARES and source region showing relative magnitudes.

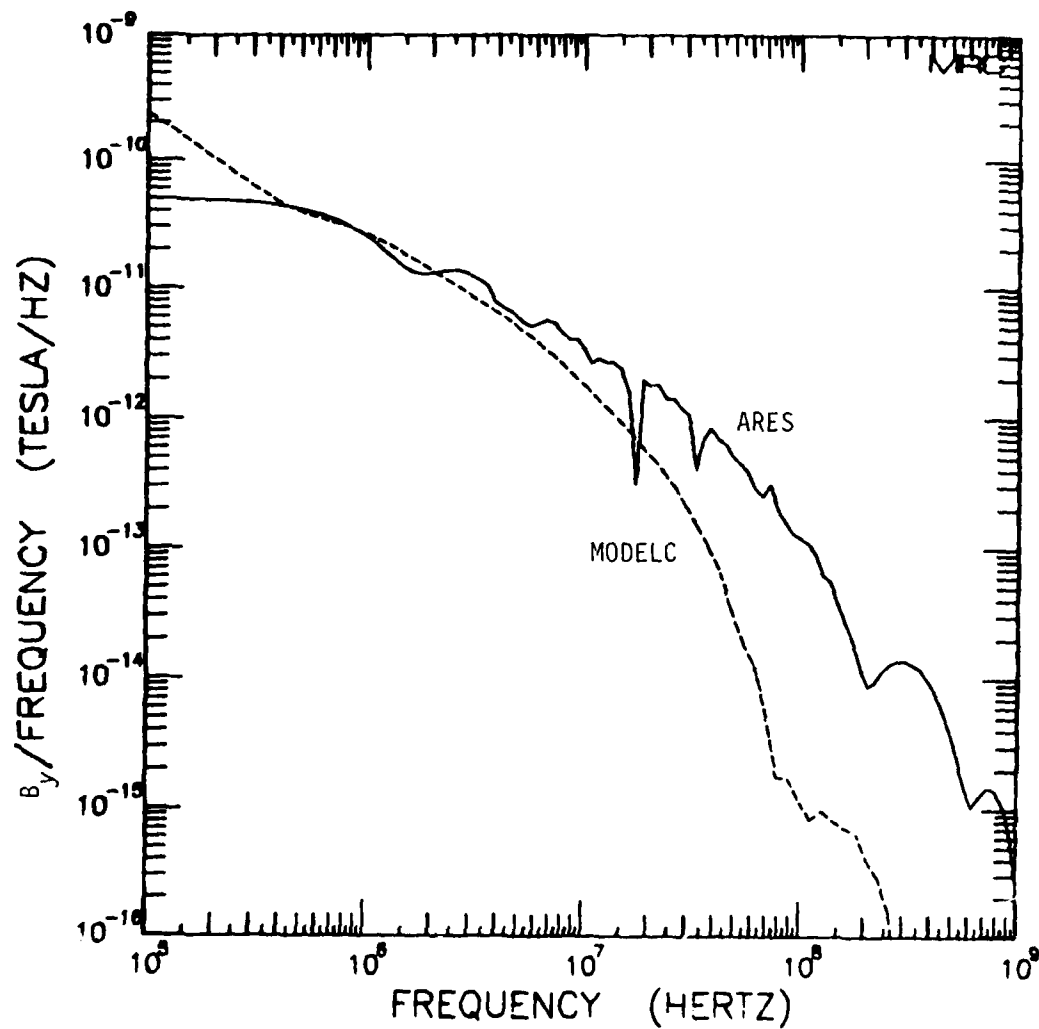


Figure 2-13. Fourier transform of magnetic field for ARES and for source region.

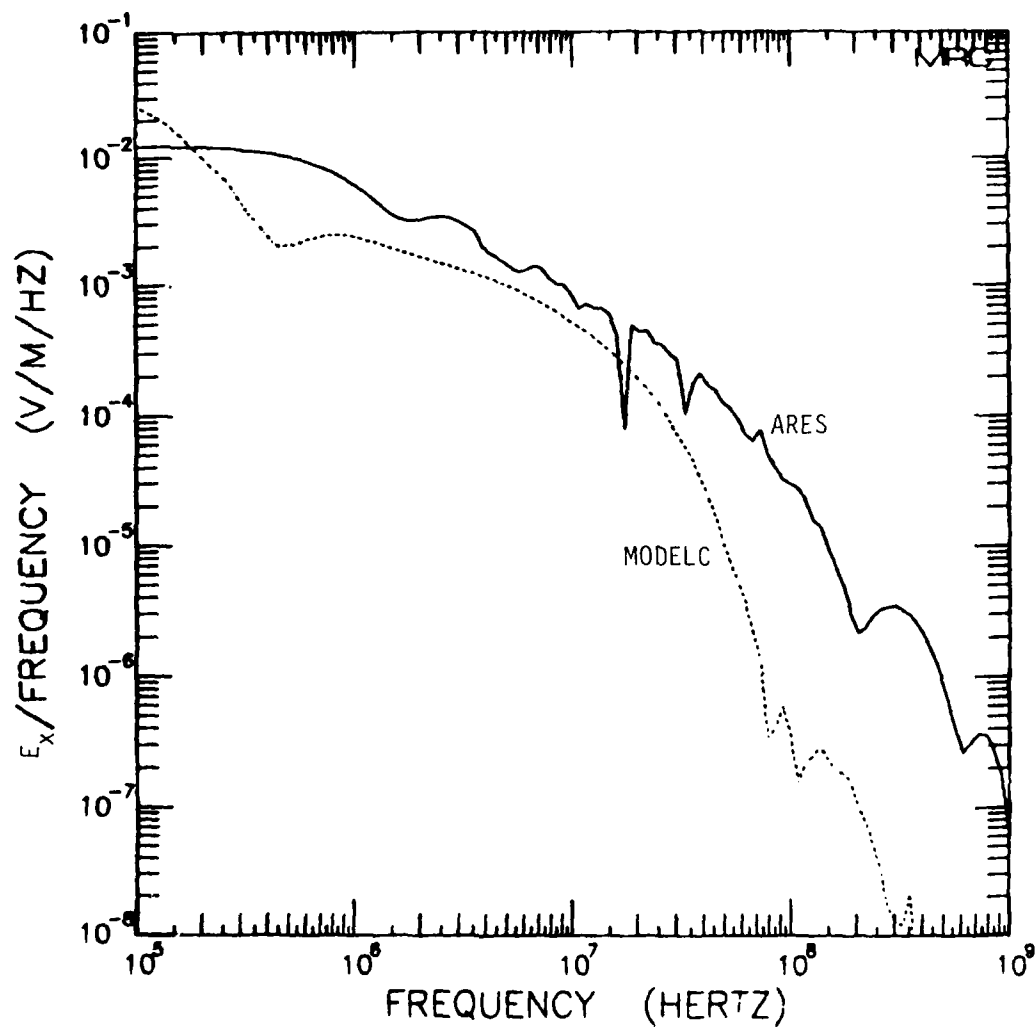


Figure 2-14. Fourier transform of vertical electric field for ARES and for source region.

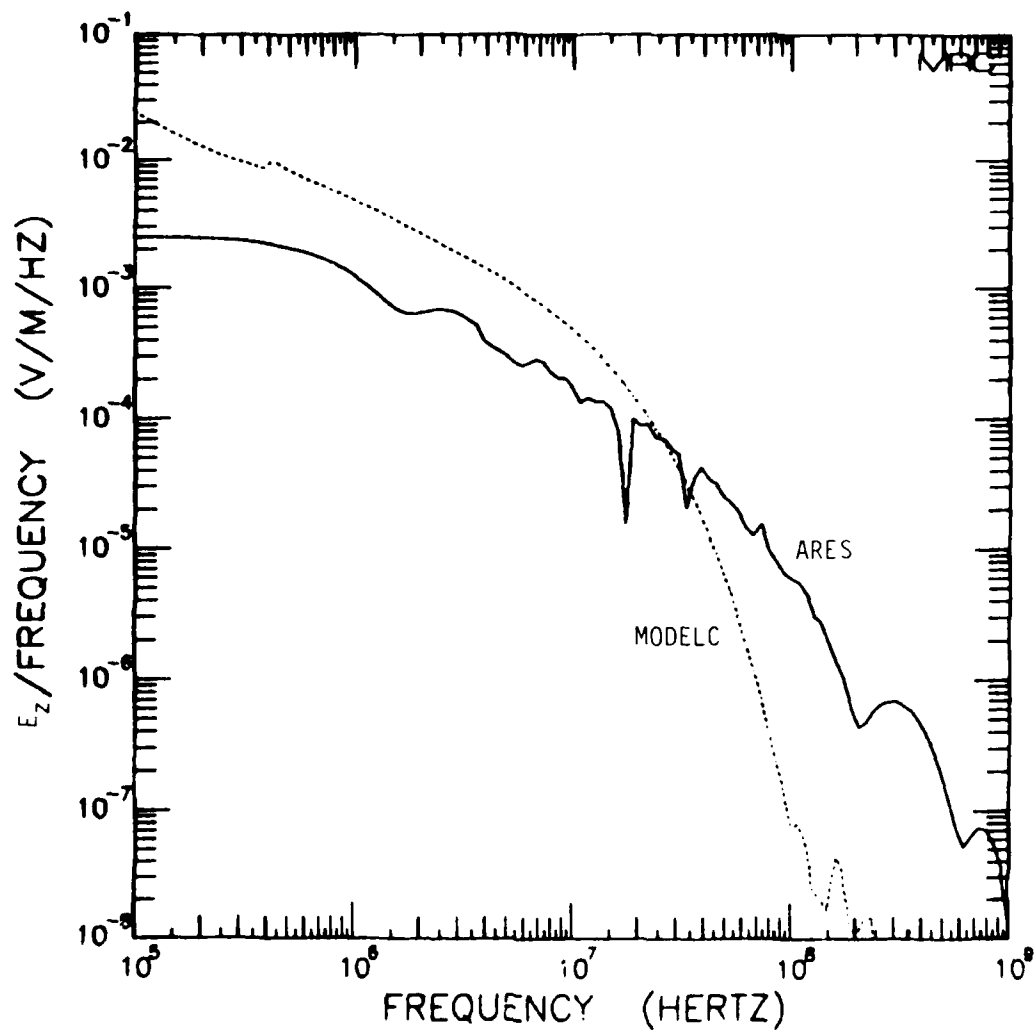


Figure 2-15. Fourier transform of longitudinal electric field for ARES and for source region.

the longitudinal electric field. It would be desirable to enhance the amplitude of the ARES  $E_z$  component. A possible means for accomplishing this is described in Section 4.

The source region contains both conduction and displacement current densities which dominate at different times. Prior to the peak of the pulse the displacement current is dominant since  $\dot{E}_x$  is large and the increasing  $\sigma$  trails  $E_x$  in time. This gives

$$\epsilon_0 \dot{E}_x \gg \sigma E_x \text{ (before peak)}$$

At the peak  $\dot{E}_x = 0$  so the conduction current is dominant giving

$$\sigma E_x \gg \epsilon_0 \dot{E}_x \text{ (at peak).}$$

For late times both  $\sigma$  and  $\dot{E}_x$  are much smaller so that both the conduction current ( $\sigma E_x$ ) and the displacement current ( $\epsilon_0 \dot{E}_x$ ) are small. They have comparable amplitudes at late times for the tactical environment selected, so

$$\sigma E_x \approx \epsilon_0 \dot{E}_x \text{ (late times)}$$

For the ARES the conduction current is zero since the air conductivity  $\sigma = 0$ . However, the ARES provides a significant displacement current density (amps/m<sup>2</sup>) as shown in Figure 2-16. For comparison the source region conduction current (labeled C) and displacement current (labeled D) are shown by dashed lines. It is seen that the ARES provides an overtest by a factor of 6 for the displacement current density.

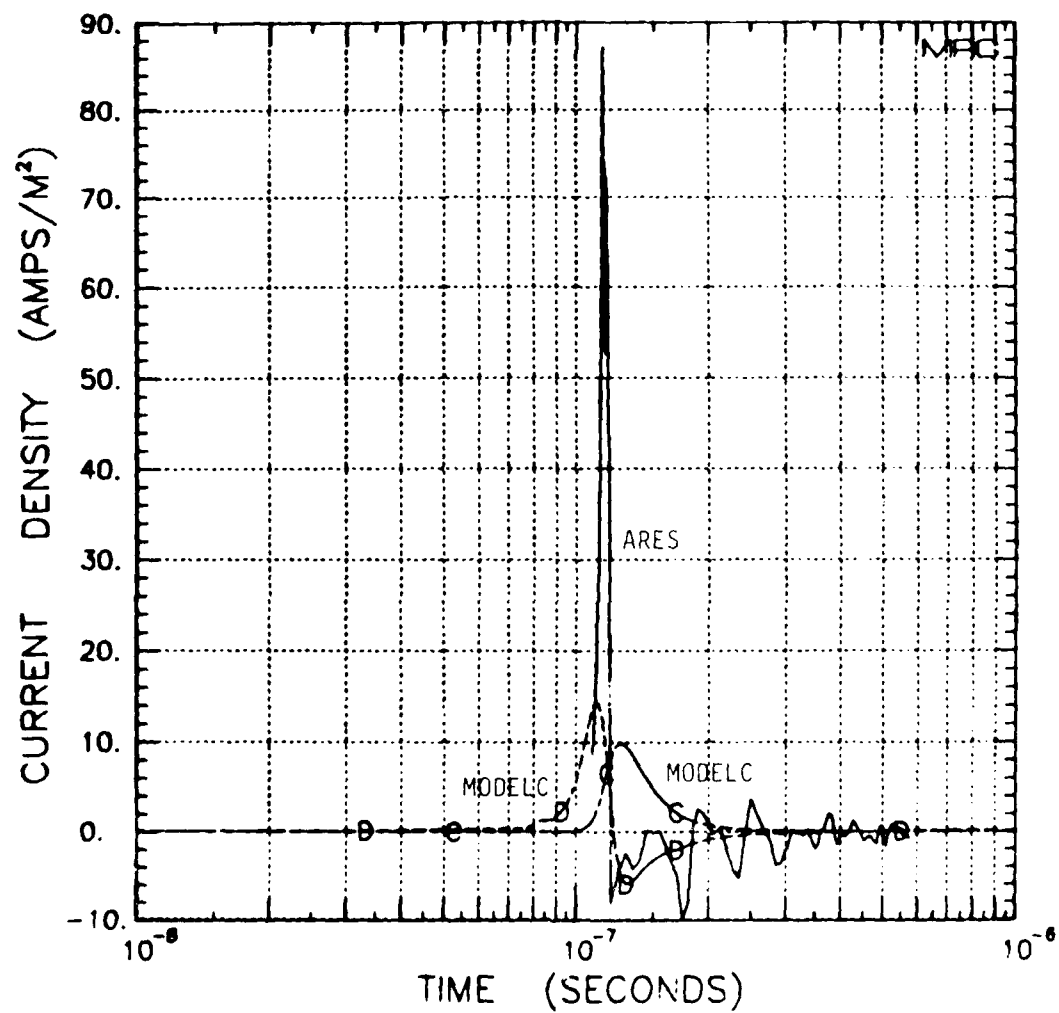


Figure 2-16. Conduction current ( $\dot{E}_x$ ) and displacement current ( $\dot{E}_x$ ) densities showing relative magnitudes. Conduction current is zero in the ARES since  $\dot{E}_x = 0$ .

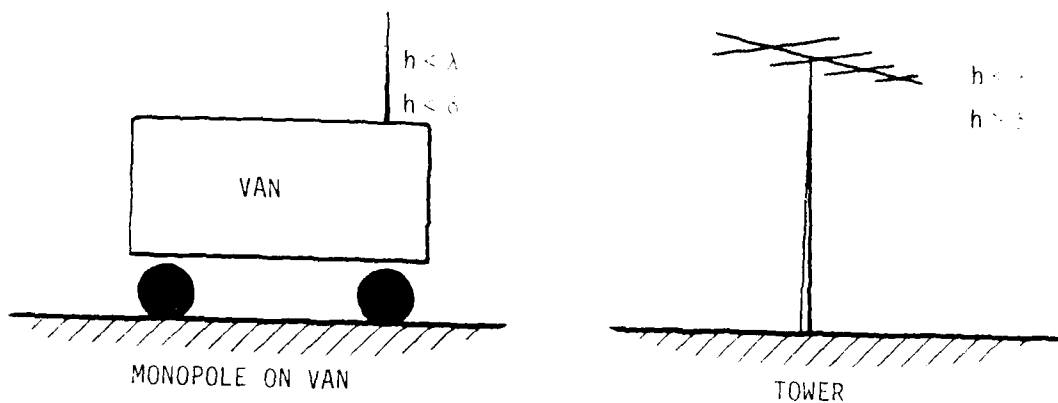
### SECTION 3

#### SOURCE REGION COUPLING

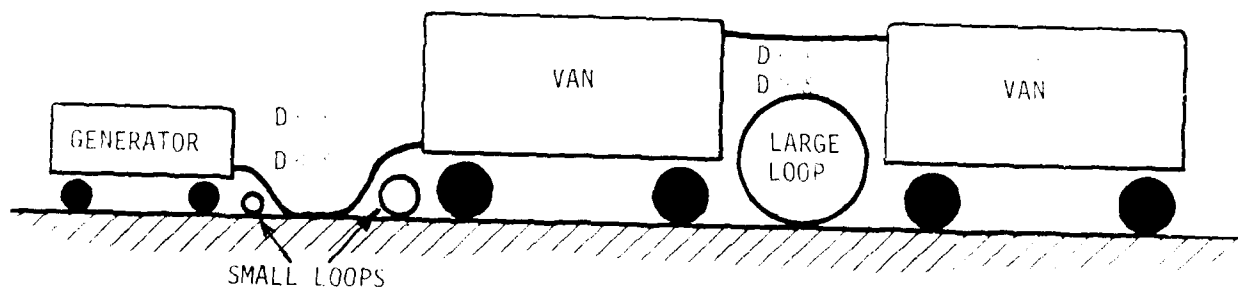
EMP coupling in the source region is characterized by a number of phenomena which are absent for plane wave coupling. These phenomena are described briefly below and their relative importance for the tactical source region (as defined in this report) is discussed.

The quantity and variety of coupling sources for a deployed tactical system is staggering; it is not possible to consider them all in this report. Broadly, however, many of the coupling mechanisms encountered may be separated into three general categories which respond to different components of the source region environment. For the tactical system these are dipoles, loops and transmission lines. While these three categories do not exhaust the possibilities for coupling into a large system, they do represent three very important and common coupling mechanisms. Some typical examples are shown in Figure 3-1. Examples of dipoles (or monopoles) are whip antennas on vans, trucks, etc., towers supporting lines or other antennas, or virtually any vertical conductor. For loops we find actual loop antennas; small loops formed with ground cables running between vans; and larger loops formed by two or more vehicles, the ground, and cables strung above ground between the vehicles. For transmission lines we find the numerous power cables, phone lines, R cables, etc., strung between all elements of the deployed system on or above the ground.

# ANTENNAS



## LOOPS



## TRANSMISSION LINES

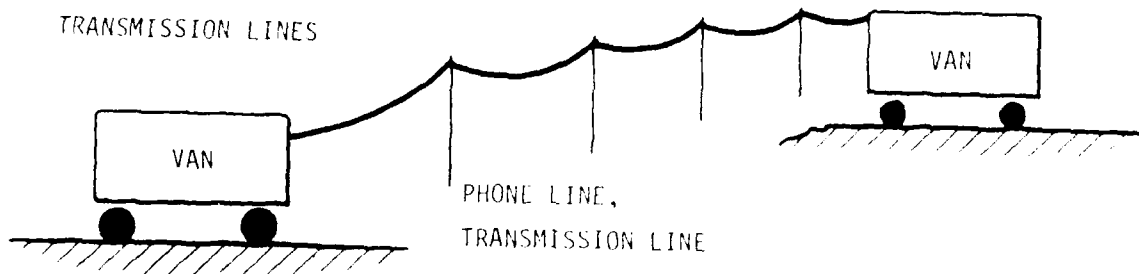


Figure 3-1. Typical coupling elements for deployed tactical systems.



We have elected to compute the response for typical examples of two of these components. These "canonical" objects are a short monopole over a ground plane and a small loop. These objects will display representative responses to the environment defined previously. The relative importance of some parameters, such as air conductivity, in determining the overall object response shall also be examined briefly.

### 3.1 COUPLING MODIFICATION IN THE SOURCE REGION ENVIRONMENT

Distinct from plane wave coupling, the source region introduces several new phenomena into the coupling picture. In this section we shall simply list the important parameters with a brief description of their impact on the general coupling environment. More detailed descriptions of source region coupling for specific objects are presented in the next sections. It is important to note that it is not necessary to accurately duplicate all aspects of the tactical environment. Rather, it is only necessary to reproduce those aspects of the environment which are important in determining the coupling response of the system. The importance of the various new parameters will be discussed below.

Parameters present in the source region which are absent for plane wave coupling are:

- (a) Direct drive from gamma radiation
- (b) Compton current
- (c) Air conductivity
- (d)  $E_0 \neq cB_\phi$
- (e) Radial electric field,  $E_r$
- (f) High field amplitudes for late times ( $t > 10^{-6}$  seconds)

The impact of these additional coupling mechanisms is most severe for ranges close to the burst (say  $< 1000$  meters). For greater ranges the impact is not so great and, in fact, at sufficiently large distances ( $> 2000$  meters) these parameters become insignificant and the EMP

disturbance is approximately a plane wave as described in Reference 1. In this report we have selected an intermediate range. Therefore each of the phenomena listed above must be examined separately to determine its relative importance.

At ranges close to the burst, objects will be subjected to large doses of gamma radiation and Compton current. These objects may then collect charge directly from the environment. The amount of charge collected depends on the relative transparency of the various objects to gamma rays, i.e., how well gamma radiation penetrates without attenuation. An object which stops all incident radiation (opaque or  $\gamma$ -thick) will simply collect all the Compton current which strikes it, acquiring a net electric charge.

Objects which are transparent ( $\gamma$ -thin) to incident gamma radiation accumulate little net charge. Gamma rays traverse the object with essentially no attenuation causing a Compton current to flow off the back of the object. This current draws away the charge resulting from the collection of Compton current on the front. Another way to view this is to regard the gamma-thin object invisible, i.e., the Compton current passes directly through the object, or is continuous through the object interfaces. In fact, gamma thin objects may still collect about 10 percent of the incident Compton current, due to material differences.

The criterion for gamma-thick or gamma-thin is given by Longmire<sup>11</sup> in terms of the projected mass of the object in the direction of the incident gamma radiation. This value of projected mass per unit area is  $m_\gamma = 30 \text{ gm/cm}^2$ . Thus an object will be gamma-thin or gamma-thick if its projected mass per unit area is small or large compared to  $30 \text{ gm/cm}^2$ . It is expected that essentially all components of a tactical system will be relatively gamma-thin. Possible exceptions are vehicle engine blocks, armored portions of vehicles or solid propellant sections of larger missiles.

To obtain some estimate of direct effects for gamma-thick objects consider the charge accumulated on a solid sphere of 1 meter radius  $R$ . The charge is obtained approximately as the peak Compton current times the half width of the pulse. This gives

$$Q = J_c \Delta t \text{ Area} = \left(19 \frac{\text{amp}}{\text{m}^2}\right) (2.5 \times 10^{-8} \text{ sec}) (\pi R^2 \text{ m}^2)$$

$$= 1.5 \times 10^{-6} R^2 \text{ Coul.}$$

For a radius  $R$  the capacitance of a sphere to infinity is

$$C = 1.11 \times 10^{-10} R \text{ farad}$$

so that the potential to infinity is

$$V = \frac{Q}{C} = \frac{1.5 \times 10^{-6}}{1.11 \times 10^{-10}} R$$

becoming  $\approx 13,500$  volts for a sphere with a 1 meter radius. This might be representative of an ungrounded vehicle with an armored cab about six feet across. The electric field which corresponds to this potential (several thousand volts/meter) will affect any antennas mounted on the vehicle. In addition, a sizeable current will flow on the surface of the vehicle as surface charges form to accommodate the electric field, and these surface currents will couple into exposed cabling. Note however that direct interaction is only significant for dense objects with an appreciable cross sectional area.

For gamma-thin objects similar calculations<sup>11</sup> indicate small fields, and currents which are fractions of an amp. Virtually all elements of a tactical system, vans, antennas, cables, electronic equipment, etc., are expected to be gamma-thin. In situations where a question exists a separate calculation should be conducted to define the expected effects. Possible methods for simulating direct interaction in ARES will be discussed in Section 4.

The range selected in this report represents the inner edge of the tactical source region. Peak air conductivity is moderately low ( $\sim 10^{-4}$  mho/meter) but not negligible and local gamma radiation levels are too low to cause significant charging of typical antennas through direct interaction.

### **3.2 COUPLING TO CANONICAL OBJECTS**

#### **3.2.1 Short Monopole Antenna**

We first consider source region coupling to the short monopole. Outside of the source region the environment can frequently be characterized by a current and/or voltage source which drives an equivalent circuit representation of the antenna. The parameters in this circuit are fixed in time. In the source region the effects of air conductivity, Compton current, volume space charge, X-rays and neutrons complicate the situation considerably.

Air conductivity is often treated in an equivalent circuit approach by introducing a time-varying resistance into the antenna equivalent circuit. The collection of Compton current is modeled by introducing an additional current source into the circuit. Results of experiments in AURORA<sup>12</sup> confirm the validity of these changes to the

normal equivalent circuit treatments of the coupling problem, at least for simple geometries.

A Thevenin equivalent circuit for the short monopole antenna is presented in Figure 3-2. Note that for the antenna to be electrically small it must not only be small compared to the wavelength of the exciting electric field, it must also be small compared to the skin depth in the ionized air produced by the burst. The skin depth in the air is given approximately by

$$\delta = \sqrt{\tau/\mu_0\sigma} \quad (3-1)$$

where  $\tau$  is a characteristic time, and  $\mu_0$  is the permeability of free space ( $= 4\pi \times 10^{-7}$  henrys/meter). For the 1.2 km environment  $\tau = 10^{-8}$  sec and  $\sigma = 3.5 \times 10^{-4}$  mho/meter so that  $\delta \approx 5$  meters. The EMP frequency content is essentially all below 100 MHz so the wavelength is greater than 3 meters. Therefore, we may select a monopole height  $h = 1$  meter as truly short in terms of both criteria. For antenna lengths which exceed 5 meters the ARES would excite an incorrect response. For intermediate antenna lengths, i.e., where the antenna length exceeds the exciting wavelength but not the skin depth, or vice versa, it would be necessary to determine the response on a case by case basis.

In Figure 3-2 the current source is proportional to the dose rate,  $\dot{D}$ , and represents the collection of Compton current for gamma-thick objects. The short monopole, however, is gamma-thin and the current source is absent from the circuit.

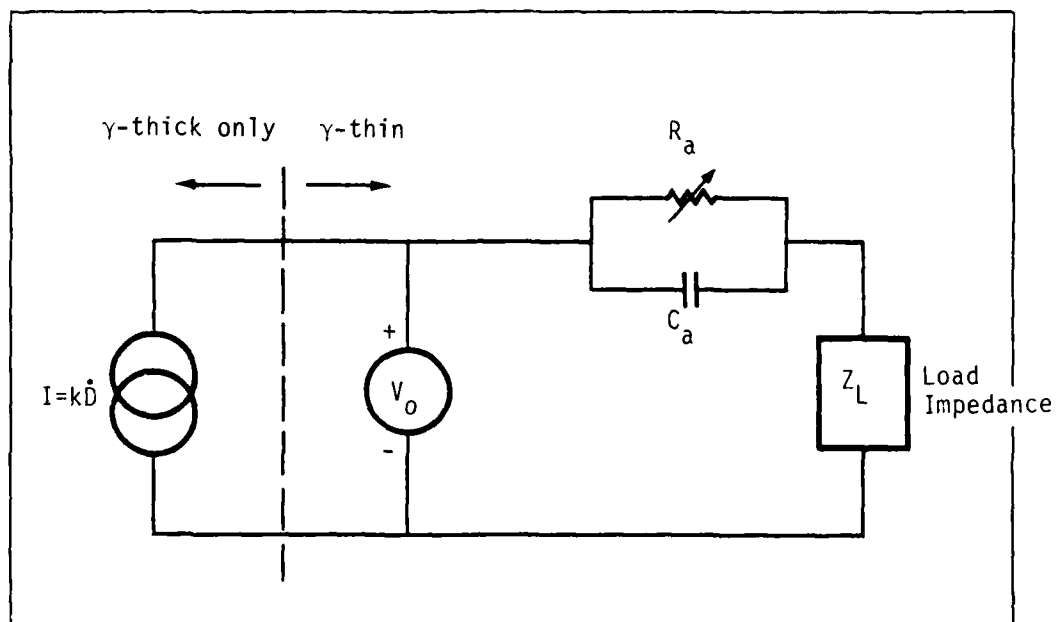


Figure 3-2. Equivalent circuit for short monopole in the source region.

The antenna capacitance is that appropriate for a thin cylinder resting on a conducting ground plane,<sup>13</sup>

$$C_a = 2h/cZ_o , \quad (3-2)$$

where

$$Z_o = 60 (\Omega - 3.39) \quad (3-3)$$

and

$$\Omega = 2 \ln(2h/a) . \quad (3-4)$$

In these expressions "h" is the height of the monopole and "a" is the radius. The shunt resistance is related to the time varying air conductivity and the antenna capacitance by

$$R_a = \epsilon_0 / C_a \sigma, \quad (3-5)$$

where  $\epsilon_0 (= 8.854 \times 10^{-12}$  farads/m) is the permittivity of free space. The voltage across the antenna and its load is

$$V_0 = - \frac{1}{2} h E_x \quad (3-6)$$

For  $h = 1$  m,  $a = 0.01$  meter we obtain  $\omega = 10.59$ , giving  $C_a = 15.4$  pf for this monopole. The short circuit current is related to  $V_0$  by

$$I_{sc} = \frac{h C_a}{2} \left[ \dot{E}_x + \frac{\sigma}{\epsilon_0} E_x \right] \quad (3-7)$$

which expresses the current in terms of environment parameters. Note that  $\epsilon_0 \dot{E}_x$  represents the displacement current and  $\sigma E_x$  the conduction current. In the source region environment the two terms dominate at different times. The displacement current is dominant during the rise of the pulse with the conduction current dominant at the peak. At late times the two current densities are comparable.

The monopole response has been computed for the "typical" environment defined earlier using the MODELIC computer code. A 50 ohm load impedance was assumed as representative of a typical load. The output

from the code is the voltage across and the current through the load impedance.

The computed monopole response is presented in Figure 3-3 for a range of 1.2 km, with and without air conductivity. This comparison shows the effect of air conductivity on the coupling. The short circuit current is presented and it is seen that air conductivity increases the peak current about 20 percent. Without air conductivity there is a large negative overshoot after the peak which is greatly reduced when conductivity is present. This behavior is easily understandable in terms of short antenna theory. Near the negative peak the displacement current and conduction current add together so conductivity enhances the response. After the peak the conduction current opposes the displacement current so the negative overshoot is reduced. In neither case is the difference very large.

For the case of no air conductivity, as in the ARES, a bipolar pulse is seen to result. For an antenna terminated in a capacitor this pulse will initially charge and then discharge the capacitor, leaving little net charge at the end of the pulse. With air conductivity present discharging does not occur and a net charge remains on the capacitor at the end of the pulse. It should be noted however that the major EMP stress on the capacitor occurs during the initial charging, and this stress is essentially the same for both cases. Thus the ARES can provide the appropriate peak stress on a major component, though this stress will not be maintained. Any system hardened to one of the waveforms would probably provide sufficient safety margin to be hard to the other. The voltage waveform shows a very similar response with the peak value increased about 15 percent with conductivity present.



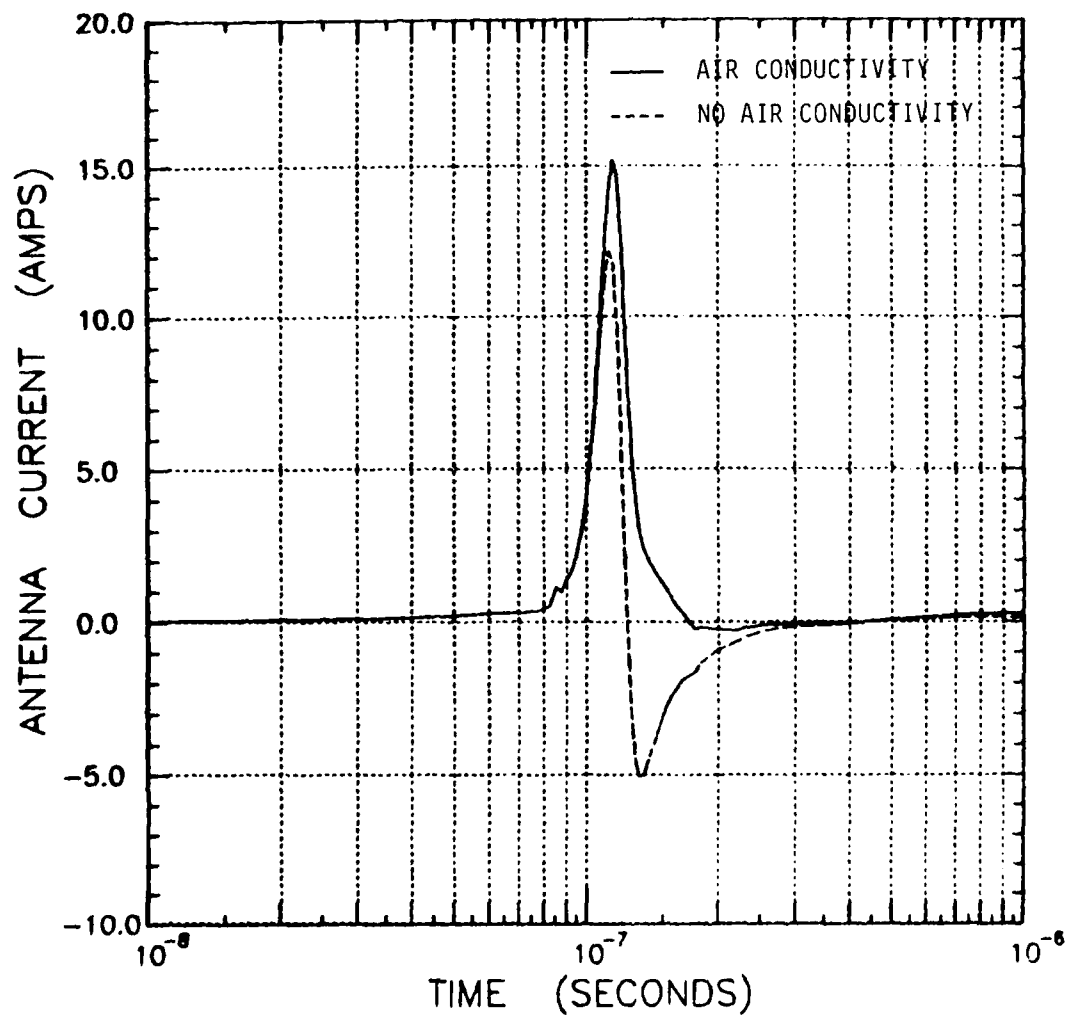


Figure 3-3. Response of a short antenna 1.2 km from a 50 kt surface burst.

For purposes of comparison similar calculations are shown in Figure 3-4 at a range of 2.0 km. Results with and without conductivity are shown. The peak current has dropped to about 2 amps. The response with and without conductivity are essentially the same so the effect of conductivity has become insignificant.

Figure 3-5 shows a comparison of the short monopole response in the ARES and in the source region with air conductivity. For a high impedance monopole, responding to  $\dot{E}$ , the ARES is seen to overdrive the short antenna by a factor of 6. A peak antenna current of 87 amps is obtained compared to 15 amps for the source region response. This provides ample safety margin for the test of all components with comparable areas exhibiting a dipole behavior. A negative overshoot is also present in the ARES response since the source region dampening provided by air conductivity is not present. A negative overshoot is also present in the ARES response since the source region dampening provided by air conductivity is not present. In the same environment, a low impedance monopole would act to integrate  $\dot{E}$  so that it would respond primarily to  $E_x$ , the vertical electric field. For this case the ARES would overdrive the antenna about 70 percent in the region of the peak, but would substantially underdrive the monopole at late times.

### 3.2.2 Small Loop Antenna

In a deployed tactical system the myriad cables, phone lines, etc., will inevitably, together with vans, vehicles, and the conducting ground, form conducting loops. These various loops will frequently be oriented with the plane of the loop perpendicular to the ground. This is an ideal arrangement for coupling to the  $B_y$  component of the source region fields. The loops will in general be small for the frequencies in

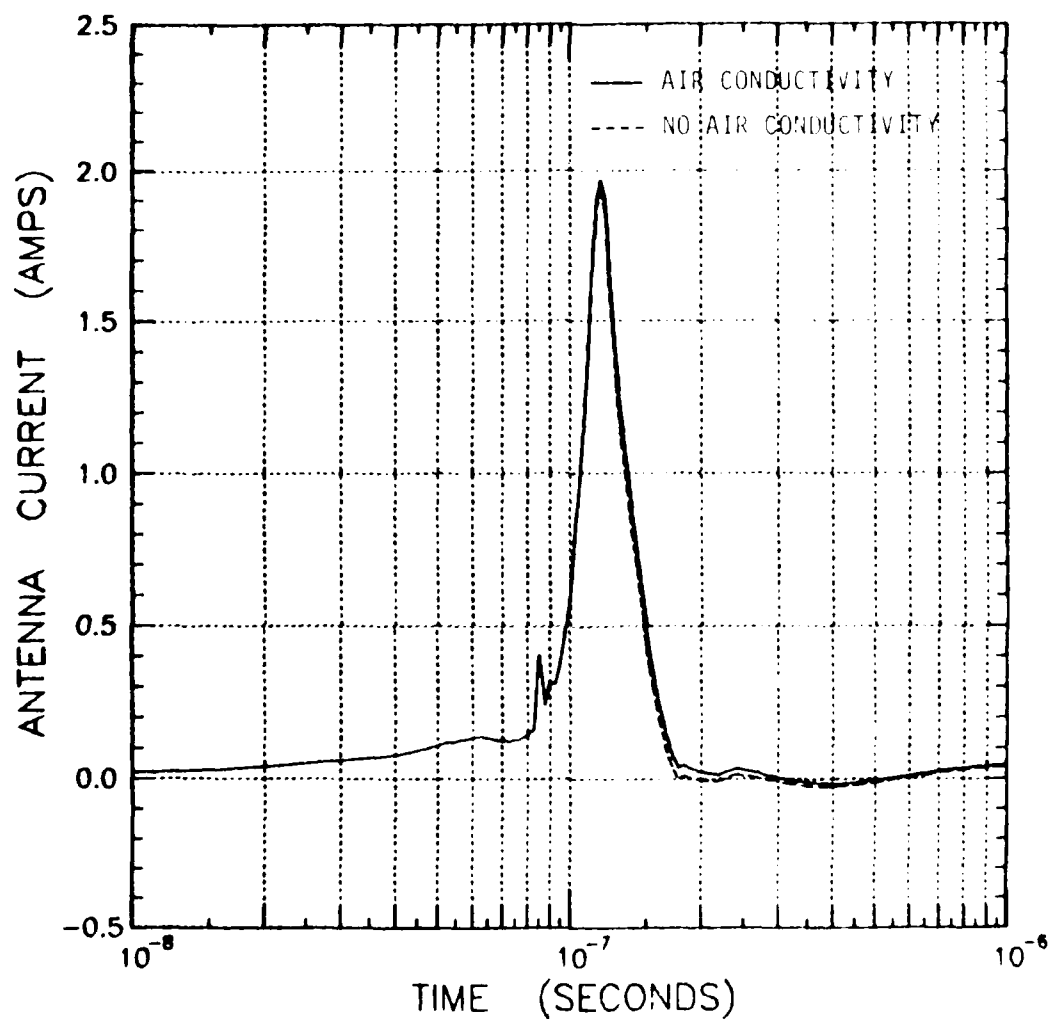


Figure 3-4. Response of a short antenna 2.0 km from a 50 kt surface burst.

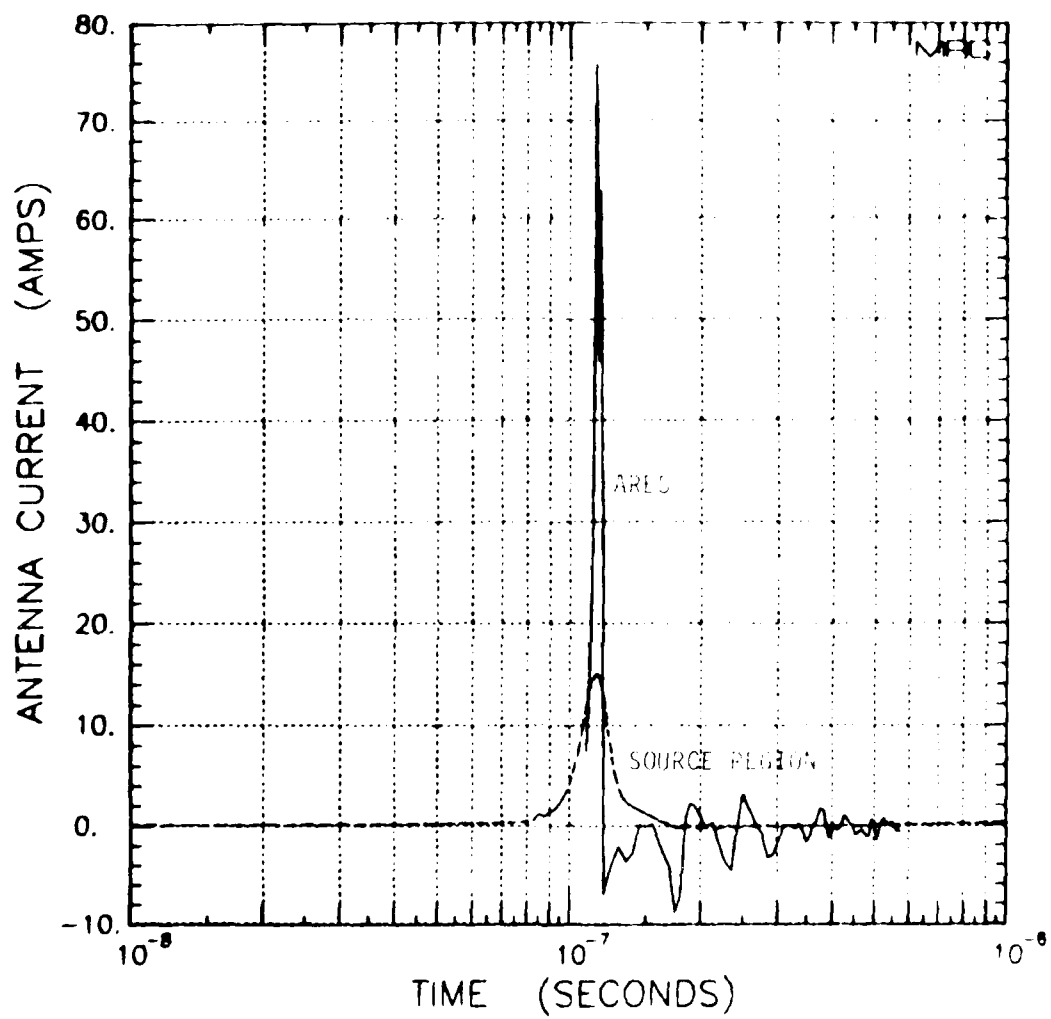


Figure 3-5. Comparison of short antenna response to ARES and source region environment.

the EMP pulse. The loop must also be small compared to the plasma skin depth,  $\delta = 5$  meters, so that the magnetic field does not change significantly over the area of the loop.

A Thevenin equivalent circuit for a small loop is presented in Figure 3-6. Again, the current source represents the collection of Compton current for gamma-thick objects, and is absent for the case being considered. Note that the resulting equivalent circuit is the same as that obtained for plane wave coupling. The air conductivity has no impact on a loop since a magnetic dipole does not respond to changes in the dielectric constant. The corresponding parameter for a loop is the permeability  $\mu$  which in general is constant, and is usually equal to  $\mu_0$ , the free space value.

For a loop of radius  $R$  with wire radius  $a$  the inductance is (for  $R \gg a$ )<sup>17</sup>

$$L_d = \mu_0 R \ln(8R/a) - 2 \text{ henrys} \quad (3-8)$$

The open circuit voltage is given by

$$V_{oc} = \dot{B}_y \dot{A} \quad (3-9)$$

for  $\dot{B}_y$  normal to the plane of the loop. For example, consider a loop with  $R = 0.564$  m. We obtain a loop area of  $\dot{A} = 1$  m<sup>2</sup>. With  $a = .01$  the loop inductance is  $L_d = 2.177$  henry. The open circuit voltage for the loop is given by equation 3-9 which expresses the antenna response in terms of the relevant EM field parameter,  $\dot{B}_y$ , the time changing magnetic field.

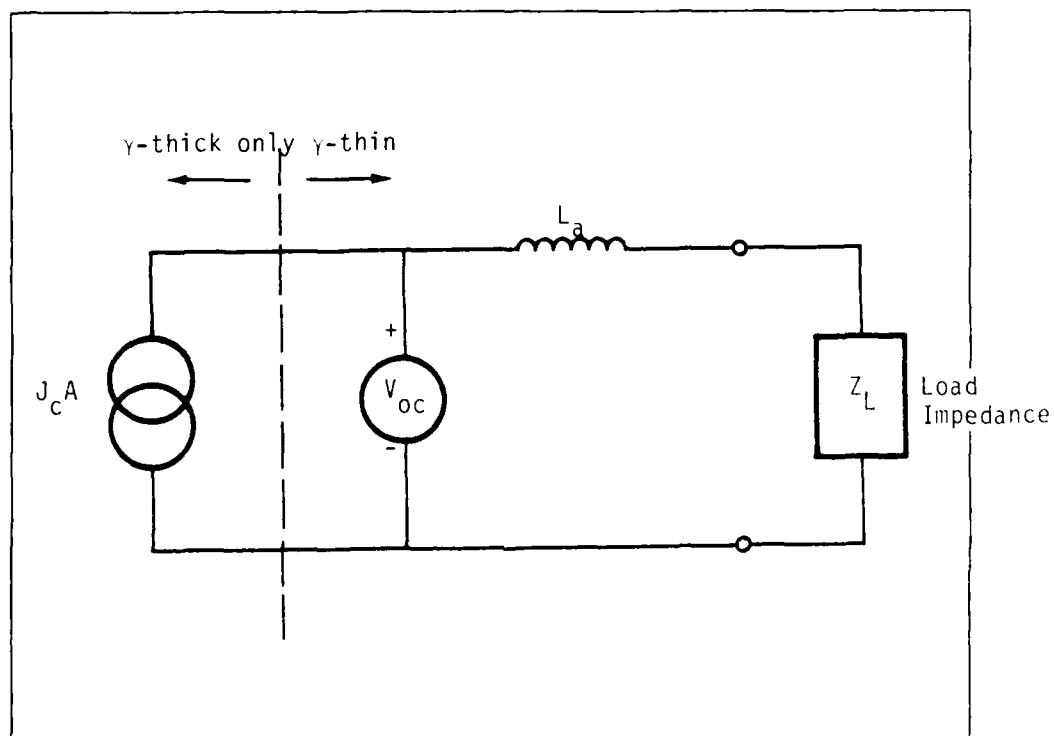


Figure 3-6. Equivalent circuit for small loop in the source region.

Figure 3-7 shows the response of a small loop in the ARS and in the source region. Since the loop area was conveniently selected as  $1 \text{ m}^2$  this figure appears identical to the  $B_y$  time derivative shown in

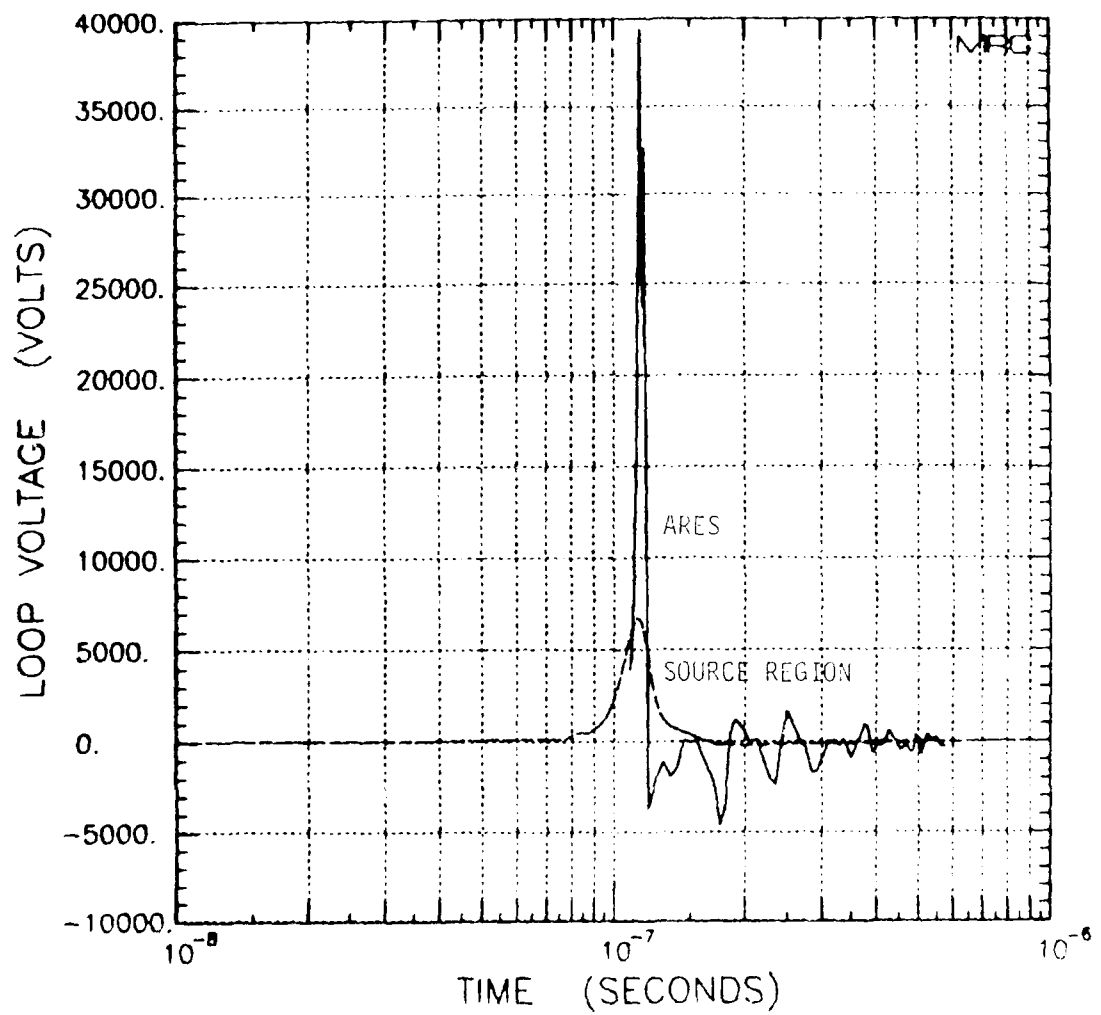


Figure 3-7. Comparison of small loop response in ARES and source region environments.

Figure 2-12. For a high impedance loop the response is to  $\dot{B}_y$  and the peak amplitude in the ARES is 39,000 volts compared to 7000 volts in the source region, so the loop is overdriven by about 6 times. However, a low impedance loop integrates  $\dot{B}$  so that it responds essentially to  $B$ . In this case the ARES would provide a valid test at the peak of the pulse but would underdrive the loop substantially at late times.



#### SECTION 4

#### ARES MODIFICATIONS FOR SOURCE REGION TESTS

The purpose of this effort is not to redesign the ARES, but rather to estimate the quality of a source region simulation in ARES. It appears, however, that some improvement in this simulation might be achieved by installing some simple, and reversible, modifications in the ARES facility. It is important that any changes remain reversible since the ARES shall be required as a plane wave simulator for the MX program in 1983 and 1986. Also, some modifications may be accomplished on the equipment under test rather than on the test facility. The following paragraphs describe the important concept of simulation fidelity and provide some specific suggestions for improving the fidelity of a source region simulation in the ARES.

Simulation fidelity is a measure of the degree to which the simulator produces a response in a test object that is relatable to the threat response. From this viewpoint there is a complementary relation between simulator realism on the one hand and theoretical understanding with calculational ability on the other. In one limit a totally realistic reproduction of the threat environment would produce a representative response, and no understanding is required (except to relate the results to another threat). At the other limit, if it is possible to calculate the response with adequate confidence, no test is required. The key to evaluating simulation fidelity is an appreciation of what is being

simulated, and what assumptions are required to relate the results to a threat exposure.

As discussed in previous sections the phenomena that distinguish SREMP from free-field EMP are:<sup>14</sup>

- (1) Air conductivity (time-varying).
- (2) Compton currents, with material interface effects.
- (3) Ionization effects in electronics, whereby the impedance presented to input/output wires is changed.

The most realistic simulation would produce the correct time-dependent gamma dose rate, with a spectrum that produces the correct absorption coefficient and Compton-current densities. If only the air conductivity is important, the requirement on the spectrum can be relaxed to producing the correct dose-rate history in air only. If the time dependence of the air conductivity is not critical the rise time of the ionization source can be increased, so that the dose rate at the time of interest (when the EM field is applied) is correct. If the relation between dose rate and air conductivity is completely unimportant, the air conductivity could be simulated by immersing the test object in a volume conducting medium (e.g., conducting foam). At this stage, one can also conceive of simulating the net Compton currents by adding appropriate high-impedance pulsed current sources connected directly to the test object.

This discussion illustrates the basic concept of simulation fidelity: a tradeoff between simulation realism and understanding. Each element of understanding simplifies the simulation problem, either by making a parameter irrelevant or producible by simpler simulation.

The definition of the source region adopted for this report permits a significant relaxation of simulator requirements for testing. It has been seen that pulse risetime and peak field values in the ARES already provide a quite good representation of the source region. Late time histories are not duplicated but neither are they as important in many cases. Source region simulation in the ARES may be further improved by adopting one or more of the following techniques:

- (a) Soil on the ARES floor
- (b) Conducting foam
- (c) Auxiliary pulsers
- (d) Current injection
- (e) Direct cable drive

None of these methods involve any direct modification of the ARES facility and only (a) requires an extended time frame (at least several months) to justify the effort involved.

A simple technique for obtaining a more realistic simulation of ground effects involves covering the ARES floor space with soil to a depth of about 4 meters. Elements of the tactical system are then deployed on the soil and tested with an actual air-ground interface. Presence of the soil would also serve to enhance the horizontal electric field ( $E_z$ ) giving a higher peak value more in line with the computed radial field. Also, if the soil surface is inclined in the z-direction from front to rear, cable drives will be enhanced since they will also be driven by a portion of the  $E_x$  field component. Remapping of the fields would be required in the ARES working space to validate values which are predicted beforehand. The movement of this large quantity of soil involves a substantial effort but is not terribly significant with a time frame of

years between installation and removal. The floor ground plane may be protected by plastic sheets.

Systems with electronic components will be affected by the photons and neutrons present in the source region. These effects need to be included in an overall coupling analysis since TREE effects can affect the coupling of the system to the environment by, for example, modifying the input impedance. Possible synergisms between EMP and TREE effects are another area where the source region is different from the free-field environment. If pre-test predictions indicate that certain system elements are particularly sensitive to radiation, a local ionization source may be introduced.

Other circumstances which call for local radiation involve instances where air conductivity adjacent to an object or inside a cavity produce a significant modification of the object response. It would then be desirable to reproduce the local air conductivity in the larger system simulation.

If the time dependence of the air conductivity is unimportant it may be simulated by immersing the test object in a volume conducting medium such as a conducting foam. Again, this technique is best suited for simulations on local objects such as an antenna. Immersing an entire vehicle in foam may be possible but is probably not practical. There will be many instances where air conductivity will be unimportant and its simulation may be dispensed with altogether.

Supplementary field excitation of particular objects might be required for some simulations. Auxiliary pulsars might be employed to enhance or modify the field environment provided by the ARES. Such units

represent common technology but would require a special installation for each test. It has been suggested<sup>15</sup> that an auxiliary pulser may be employed to simulate the late time fields present in the source region. This pulser would possess a slow rise time and would tend to "fill in" at the end of the ARES pulse.

As previously discussed some components of the deployed system could be gamma-thick, e.g., an armored vehicle. These components will incur a net electric charge in the source region environment resulting from direct interaction. This direct interaction may be simulated by current injection directly onto the object of interest. Sources and feed lines could be buried in the soil with minimum affect on the simulation. Pulse risetimes and peak amplitudes are readily within the state-of-the-art.

Another instance where direct drive might be useful is the accumulation of current for long cable runs. Simulation of currents induced on long runs associated with particular equipments may be accomplished by allowing the cable to exit the ARES working volume. Direct drive might then be accomplished with equipment exterior to the ARES facility.

Testing of internal interaction effects on system components such as vans cannot be accomplished in the ARES and must be handled in other simulators, such as AURORA, which are designed to produce an X-radiation environment. Some related work has already been performed.<sup>16</sup> Testing in other simulators will serve to compliment the ARES to provide a more thorough evaluation of the entire system response.

## SECTION 5

### SUMMARY AND CONCLUSIONS

The previous sections have defined a tactical source region environment and made comparisons with the environment provided by the ARES. Coupling of both EMP environments into specified canonical objects have been examined. In the short time span available for the current study this effort could not be exhaustive but some interesting results have been obtained. The effort presented above has emphasized EMP coupling into deployed tactical systems since the ARES appears particularly suited to the evaluation of large system components. As such, this effort has only addressed the inner edge of the tactical source region, but this represents the important region where crew survival is possible (and therefore where equipment survival is necessary).

A summary of pros and cons for the ARES as a source region simulator is presented in Table 5-1. In general it is concluded that those aspects of the source region environment which are absent in the ARES are either unimportant or may be provided on an individual basis for specific system elements. It has been shown that many important coupling elements (dipoles, loops and transmission lines) respond primarily to time derivatives of the impinging EMP,  $\dot{E}_z$ ,  $\dot{E}_x$  and  $\dot{B}_y$ . The ARES provides a significant overtest capability (about 6 times) for these time derivatives.

Table 5-1. Source region simulation using the ARES.

ARES	CONS	COMMENTS
<b>OPERATIONAL</b>		
1. Large size - capable of testing many different weapons	1. Outdoor facility - weather dependent	Large size is unique
2. Repeatedly Pulse		
3. Rapid insulator turn-around, multiple shots per day		
4. Inert, simulations can be conducted in same region		Restoration of facility to original configuration is straightforward
<b>ANALYTICAL</b>		
1. Reasonable reproduction of many important aspects of environment (inner edge of source region)	2. Absence of some significant aspects of source region environment	Various supplementary sources would be required to provide absent parameters for particular objects and tests.
<ul style="list-style-type: none"> <li>a) Pulse rise time</li> <li>b) Peak field amplitudes</li> <li>c) Correct field components present with correct sense</li> <li>d) Reasonable representation of frequency spectrum</li> <li>e) Part of exceed source energy values</li> </ul>	<ul style="list-style-type: none"> <li>a) radiation &amp; neutrons</li> <li>b) Compton current</li> <li>c) air conductivity</li> <li>d) late time high field amplitudes</li> </ul>	Provides overttest capability for dipole and loop responses

Table 5-1 (continued).

PROS	CONS	COMMENTS
6. Can test wide range of devices	3. Fields not uniform over entire working volume	Fields also not uniform in source region; not a problem if fields are known
	4. Frequencies not tested $\approx 17$ MHz plus multiples	Environment a strong function of crew survival (rather than of device characteristics per se)
7. Air ground interface can be reasonably represented	5. Power consumed for lingering source region pulse not represented	Requires placement of earth on working volume floor
	6. Cannot test effects on unmanned system components located closer to burst	



The important air-ground interface may be included in ARES tests by the simple expedient of covering the ARES working floor space with earth. Where air conductivity is deemed important it may be provided by using conducting foams around particular system elements. Direct current injection might also be employed on some objects to supplement the environment provided by the ARES. It appears that any modifications necessary to supplement the ARES environment may be accomplished directly on the test objects or within an earth covered floor space without impact on the ARES facility proper.

Recycling time for the ARES pulser is only three minutes while the entire facility may be recycled in about five minutes. This provides a significant advantage when compared with such source region facilities as AURORA which require much longer recycle times (2 hours). Costs for both facilities appear comparable, but the ARES could provide considerably more data for a given test period.

It is suggested that further study be performed to provide firm recommendations for an ARES source region test facility. A specific system should be selected and examined in detail. This approach would result in firm suggestions for modifications to supplement the environment provided by the ARES. In particular, it is necessary to examine the effect of soil on the ARES floor space.

In closing, we firmly agree with the following quote from the ARES facility User's Manual<sup>17</sup>:

"The data obtained through experimentation at ARES are necessarily only a portion of the information eventually required for an assessment of the EMP vulnerability and survivability on any system. The ARES Facility is not can stand alone, unsupported by analysis and other test efforts. As a general rule, a comprehensive assessment program should be well under way before an attempt is made to design the experiment to be conducted at ARES.

Such an assessment program will include identification and ranking by relative importance of all paths of entry of electromagnetic energy into the weapon system, identification of the critical circuits within the system, determination of the environment parameters requiring close reproduction during test and analysis of the coupling paths within the system. Clearly, some test effort will have to be completed prior to designing a test program to be executed at the ARES. The preliminary testing, such as experimental verification of circuit thresholds, should be completed and understood before the ARES testing is begun.

Regardless of the type of system being tested, the yield of the experimental effort will depend on the care with which the experiment is designed and executed, especially with regard to the characteristics of the facility and the ways in which these characteristics satisfy the user's EMP requirements."

It appears that the ARES will prove to be a useful source region simulator for tactical Army systems when proper attention is focussed on the design of the test. There is merit to testing systems with small antennas in the ARES. These test results are test relatable. It is possible to test both low and high altitude susceptibility of tactical systems simultaneously, with the ARES capable of providing an overtest of many important system components.

## REFERENCES

1. Spohn, D.J., private communication.
2. Berberet, J.A. and A. Lowrey, The Approach of an EMP Hardened Tactical Army, System EMP Hardening Seminar, NOSC, San Diego, California, 7-9 August 1979.
3. Glasstone, S. and P.J. Dolan, eds., The Effects of Nuclear Weapons, 3rd Edition, U.S. Government Printing Office, 1977.
4. Longmire, C.L., On the Electromagnetic Pulse Produced by Nuclear Explosions, IEEE Trans. on Antennas and Propagation, Vol. AP-26, No. 1, January 1978.
5. Crevier, W.F., and E.D. Kalasky, Evaluation of AURORA as a Tactical Source Region Simulator, AURORA EMP Memo 21, Mission Research Corporation, Santa Barbara, California.
6. Wirth, J.C., ARES Facility Description, Facilities, Equipment and Operation, Volume I, Final Report, DNA 3265F-1, Braddock, Dunn and McDonald, Inc., Albuquerque, New Mexico, 12 March 1974.
7. Hutchins, R.L., ARES Facility Description, Electromagnetic Environment, Volume II, Final Report, DNA 3265F-2, Braddock, Dunn and McDonald, Inc., Albuquerque, New Mexico, 12 March 1974.
8. Dyche, J.W. and R.A. Kitter, ARES Facility Description, Data Processing System, Volume III, Final Report, DNA 3265F-3, Braddock, Dunn and McDonald, Inc., Albuquerque, New Mexico, 12 March 1974.
9. Preliminary, Tall Pines Field Mapping Report, BDM/IAC-79-063-TR, The BDM Corporation, Albuquerque, New Mexico, March 1979.
10. Evans, R.D., The Atomic Nucleus, McGraw-Hill Book Co., New York, 1955.

11. Longmire, C.L., Direct Interaction Effects in EMP, LAD-6-12, Los Alamos Nuclear Corporation, January 1971; also Interaction Note 88, January 1971.
12. Merkle, G., D.O. Spohn, C.L. Longmire and W.F. Grevier, An Equivalent Circuit Analysis of the HDL Concentric Cylinder Experiments in AURORA, IEEE Trans. Nucl. Sci., Vol. NS-24, No. 6, December 1977.
13. Messier, M.A., Coupling to Antennas, Chapter 10, Revised, DAA Handbook, Mission Research Corporation, Santa Barbara, CA.
14. Baum, C.E., EMP Simulators for Various Types of Nuclear EMP Environments: An Interim Categorization, IEEE Trans. Ant. and Prop. Vol. AP-26, No. 1, January 1978.
15. V.A.J. van Lint, private communication.
16. Meyer, O.L., W.L. Chadsey and V.W. Pine, Internal S&HR Response of a Communications Van to AURORA Irradiation, IEEE Trans. Nucl. Sci., Vol. NS-24, No. 6, December 1977.
17. ARES User's Manual, BDM/FAC-78-103-ER, The BDM Corporation, Albuquerque, New Mexico, May 1978.



1. *Phragmites australis* (Cav.) Trin. ex Steud.

**Abstract.**—The effects of two different types of artificial cover on the distribution and abundance of juvenile largemouth bass (*Micropterus dolomieu*) were examined in a small, shallow pond. The cover consisted of either floating plastic mulch or submerged PVC pipe. Juvenile largemouth bass were more abundant in the area containing the floating plastic mulch than in the area containing the submerged PVC pipe. This result was similar to that reported by other researchers who have found that juvenile largemouth bass prefer floating cover over submerged cover. However, the results of this study suggest that the type of cover may also affect the size of the fish. In this study, the mean length of the fish in the area containing the floating plastic mulch was significantly greater than the mean length of the fish in the area containing the submerged PVC pipe. These results suggest that the type of cover may also affect the growth rate of juvenile largemouth bass.

the 1990s, the number of people in the world who are illiterate has increased from 1.2 billion to 1.5 billion. The number of illiterate people in the world is projected to reach 1.7 billion by the year 2015. The number of illiterate people in the world is projected to reach 1.7 billion by the year 2015.

[illegible][illegible]

the 1990s, the number of people in the world who are illiterate has increased from 1.2 billion to 1.5 billion. The number of illiterate people in the world is expected to reach 1.7 billion by the year 2015. The number of illiterate people in the world is expected to reach 1.7 billion by the year 2015.

[illegible]

the 1990s, the number of people in the world who are illiterate has increased from 1.2 billion to 1.5 billion. The number of illiterate people in the world is expected to reach 1.7 billion by the year 2015. The number of illiterate people in the world is expected to reach 1.7 billion by the year 2015. The number of illiterate people in the world is expected to reach 1.7 billion by the year 2015.

the 1990s, the number of people in the world who are undernourished has declined from 1.1 billion to 800 million. The number of people who are malnourished has declined from 1.5 billion to 1 billion. The number of people who are obese has increased from 100 million to 300 million. The number of people who are overweight has increased from 100 million to 300 million. The number of people who are obese and overweight has increased from 100 million to 300 million. The number of people who are obese and overweight has increased from 100 million to 300 million.

[illegible]
$$\begin{aligned} \text{cost} &= \sum_{i=1}^n \sum_{j=1}^n |x_{ij} - y_{ij}|^2 \\ \text{cost} &= \sum_{i=1}^n \sum_{j=1}^n |x_{ij} - y_{ij}|^2 \\ &= \sum_{i=1}^n \sum_{j=1}^n |x_{ij} - y_{ij}|^2 \end{aligned}$$
[illegible][illegible]

1. *Staphylococcus aureus* (ATCC 12228) and *Staphylococcus epidermidis* (ATCC 12228) were grown in tryptic soy broth (TSB) (Difco) supplemented with 0.5% yeast extract (Difco) and 0.5% NaCl. *Staphylococcus aureus* was grown in TSB supplemented with 0.5% yeast extract and 0.5% NaCl. *Staphylococcus epidermidis* was grown in TSB supplemented with 0.5% yeast extract and 0.5% NaCl.

# DEPARTMENT OF ENERGY

Department of Energy  
Alternative Operations Office  
ATTN: WSOB  
ATTN: LTID

Department of Energy  
ATTN: Office of Utility Systems & Control

DEPARTMENT OF AGRICULTURE

Central Intelligence Agency  
ATTN: OAK-NEB

Department of Transportation  
ATTN: Civil Engineering

General Services Management Agency  
ATTN: General Eval & Eval Rep Div  
ATTN: Plans & Operations (A0)  
ATTN: Plans & Operations (B0)

General Services Management Agency  
ATTN: GIL-M, Martins

## DEPARTMENT OF AGRICULTURE CONTRACTORS

University of Kentucky National Lab  
ATTN: J. L. D. Mcken  
ATTN: J. L. D. Mcken  
ATTN: National Technical Library  
ATTN: J. L. D. Mcken  
ATTN: J. L. D. Mcken  
ATTN: J. L. D. Mcken

Los Alamos National Scientific Lab  
ATTN: M. G. L. Mcken  
ATTN: M. G. L. Mcken  
ATTN: J. L. D. Mcken

Seattle National Lab  
ATTN: R. Parker  
ATTN: L. Martin  
ATTN: J. L. D. Mcken

## DEPARTMENT OF DEFENSE CONTRACTORS

ARM Corp  
ATTN: Library

ARM Corp  
ATTN: Document Control

ARM Corp  
ATTN: M. G. L. Mcken

ARM Corp  
ATTN: J. L. D. Mcken  
ATTN: J. L. D. Mcken  
ATTN: National Technical Library  
ATTN: J. L. D. Mcken

ARM Corp  
ATTN: J. L. D. Mcken

ARM Corp  
ATTN: J. L. D. Mcken  
ATTN: J. L. D. Mcken  
ATTN: National Technical Library

ARM Corp  
ATTN: J. L. D. Mcken

## DEPARTMENT OF DEFENSE CONTRACTORS

ARM Corp  
ATTN: J. L. D. Mcken  
ATTN: J. L. D. Mcken

ARM Corp  
ATTN: J. L. D. Mcken

ARM Corp  
ATTN: J. L. D. Mcken

ARM Corp  
ATTN: J. L. D. Mcken

ARM Corp  
ATTN: J. L. D. Mcken

ARM Corp  
ATTN: J. L. D. Mcken

ARM Corp  
ATTN: J. L. D. Mcken  
ATTN: J. L. D. Mcken

ARM Corp  
ATTN: J. L. D. Mcken

ARM Corp  
ATTN: J. L. D. Mcken

ARM Corp  
ATTN: J. L. D. Mcken

ARM Corp  
ATTN: J. L. D. Mcken  
ATTN: J. L. D. Mcken

ARM Corp  
ATTN: J. L. D. Mcken

ARM Corp  
ATTN: J. L. D. Mcken

ARM Corp  
ATTN: J. L. D. Mcken

ARM Corp  
ATTN: J. L. D. Mcken

ARM Corp  
ATTN: J. L. D. Mcken

ARM Corp  
ATTN: J. L. D. Mcken

ARM Corp  
ATTN: J. L. D. Mcken

ARM Corp  
ATTN: J. L. D. Mcken  
ATTN: J. L. D. Mcken  
ATTN: J. L. D. Mcken

ARM Corp  
ATTN: J. L. D. Mcken

ARM Corp  
ATTN: J. L. D. Mcken

DEPARTMENT OF DEFENSE CONTRACTORS (Continued)

Georgia Institute of Technology  
ATTN: Res & Sec Coord for H. Denny

Grumman Aerospace Corp  
ATTN: L-01 35

Harris Corporation  
ATTN: A. Strain  
ATTN: V. Pres & Mgr Progs Div

Hazeltine Corp  
ATTN: J. Okrent

Honeywell, Inc  
ATTN: R. Johnson  
ATTN: SAC Library

Honeywell, Inc  
ATTN: W. Stewart  
ATTN: S. Graff

Hughes Aircraft Co  
ATTN: S. Walker  
ATTN: J. Singletary  
ATTN: CTOC 07110

Hughes Aircraft Co  
ATTN: A. Narevsky

III Research Institute  
ATTN: J. Bridges  
ATTN: L. Mindel

Institute for Defense Analyses  
ATTN: Tech Info Services

International Tel & Telegraph Corp  
ATTN: Technical Library

LA Physics Corp  
ATTN: H. Milde  
ATTN: R. Evans

LRI Corp  
ATTN: N. Rudie  
ATTN: B. Williams

LEGOR  
ATTN: W. Radasky

LEADON  
ATTN: R. Stahl  
ATTN: L. Wenas

LEYCOR  
ATTN: Library

Liman Sciences Corp  
ATTN: W. Ware  
ATTN: F. Shelton  
ATTN: A. Bridges  
ATTN: W. Rich  
ATTN: J. Lubell  
ATTN: N. Beauchamp

Litton Systems, Inc  
ATTN: M&A 01  
ATTN: EMC 6P

DEPARTMENT OF DEFENSE CONTRACTORS (Continued)

Litton Systems, Inc  
ATTN: J. Maggs

Lockheed Missiles & Space Co, Inc  
ATTN: Technical Information Center

Lockheed Missiles & Space Co, Inc  
ATTN: L. Smith  
ATTN: L. Rossi  
ATTN: G. Heath  
ATTN: R. Thayer  
2 cy ATTN: S. Tamuty

M.I.T. Lincoln Lab  
ATTN: L. Loughlin

Martin Marietta Corp  
ATTN: M. Griffin

Martin Marietta Corp  
ATTN: G. Freyer

McDonnell Douglas Corp  
ATTN: T. Ender

McDonnell Douglas Corp  
ATTN: Technical Library Services  
ATTN: S. Schneider

Mission Research Corp  
ATTN: LMP Group  
ATTN: W. Hart  
ATTN: D. Holst  
5 cy ATTN: Document Control

Mission Research Corp  
ATTN: A. Chodorow  
ATTN: L. McCormick

Mission Research Corp, San Diego  
ATTN: V. Van Lint

Mission Research Corporation  
ATTN: Sec Off for W. Stark

MITRE Corp  
ATTN: M. Fitzgerald

Norden Systems, Inc  
ATTN: Technical Library

Northrop Corp  
ATTN: V. Demartino  
ATTN: B. Ahlport  
ATTN: Lew Smith

Pacific-Sierra Research Corp  
ATTN: H. Brode

Palisades Inst for Res Services, Inc.  
ATTN: Records Supervisor

Physics International Co  
ATTN: Document Control



DEPARTMENT OF DEFENSE CONTRACTORS (Continued)

R & D Associates  
ATTN: Document Control  
ATTN: R. Schafer  
ATTN: B. Gage  
ATTN: P. Haas

R & D Associates  
ATTN: J. Bombardt

Rane Corp  
ATTN: LIE-D

Raytheon Co  
ATTN: G. Joshi

Raytheon Co  
ATTN: H. Flescher

RCA Corp  
ATTN: G. Brucker

RCA Corp  
ATTN: L. Minich  
ATTN: D. O'Connor

Rockwell International Corp  
ATTN: V. Michel  
ATTN: D/243-060, D31-CAS1  
ATTN: J. Monroe

Rockwell International Corp  
ATTN: B. White

Rockwell International Corp  
ATTN: B-1 Div TIC, SA08

Rockwell International Corp  
ATTN: F. Shaw

Science Applications, Inc  
ATTN: R. Parkinson

Science Applications, Inc  
ATTN: W. Chadsey

Sidney Frankel & Associates  
ATTN: S. Frankel

Singer Co  
ATTN: Technical Information Center

Sperry Rand Corp  
ATTN: Technical Library

AVCO Research & Systems Group  
ATTN: Library Ac 30

Battelle Memorial Institute  
ATTN: E. Leach

BDM Corp  
ATTN: Corporate Library

DEPARTMENT OF DEFENSE CONTRACTORS (Continued)

Sperry Rand Corp  
ATTN: D. Schow

Spire Corp  
ATTN: R. Little

SRI International  
ATTN: A. Whitson  
ATTN: B. Gaster  
ATTN: E. Vance

Sylvania Systems Group  
ATTN: L. Blaisdell  
ATTN: C. Thornhill

Sylvania Systems Group  
ATTN: J. Waldron  
ATTN: A. Novenski  
ATTN: E. Metchok  
ATTN: D. Flood  
ATTN: M. Nuretera  
ATTN: C. Ramsbottom

Systems, Science & Software, Inc  
ATTN: A. Wilson

Teledyne Brown Engineering  
ATTN: F. Leonard

Texas Instruments, Inc  
ATTN: Technical Library  
ATTN: D. Manu

Texas Tech University  
ATTN: T. Simpson

TRW Defense & Space Sys Group  
ATTN: R. Holloway  
ATTN: J. Adams  
ATTN: L. Magnolia

TRW Defense & Space Sys Group  
ATTN: R. Mortensen

Varian Associates, Inc  
ATTN: M. Jery

Westinghouse Electric Corp  
ATTN: Technical Library

Aerospace Corp  
ATTN: A. Pearlster  
ATTN: E. Perry  
ATTN: R. Taylor  
ATTN: J. Gantwerker  
ATTN: J. Westerman

Adaptation Associates  
ATTN: Library

DATE  
FILMED  
5-18